THE UNIVERSITY OF MICHIGAN

COLLEGE OF ENGINEERING

Department of Engineering Mechanics

Technical Report

A THEORETICAL AND EXPERIMENTAL STUDY OF THE STABILITY OF THIN ELASTIC SPHERICAL SHELLS

D. Beaty

ORA Project 04246

under contract with:

NATIONAL SCIENCE FOUNDATION
GRANT NO. 14475
WASHINGTON, D. C.

administered through:

OFFICE OF RESEARCH ADMINISTRATION ANN ARBOR

October 1962

This report was also a dissertation submitted in partial fulfillment of the requirements for the degree of Doctor of Philosophy in The University of Michigan, 1962.

TABLE OF CONTENTS

LIST OF ILLUSTRATIONS

LIST OF ILLUSTRATIONS (Concluded)

ABSTRACT

The investigation of the behavior of a uniformly thick, thin spherical shell subjected to uniform external pressure in the buckling and post-buckling regions is undertaken both from a theoretical and from an experimental point of view.

A perturbation scheme similar to one developed by Koiter is applied to the nonlinear buckling problem of a complete spherical shell. The nonhomogeneous linear differential equations which result are solved, with the aid of the high speed digital computer, in a finite series of Legendre polynomials. In the neighborhood of the linear buckling load, the shell is shown to be unstable both for the case of the linear buckling mode's being an odd function about the equator and for its being an even function.

Four hemispherical shells made of materials with low Young's moduli (less than 1000 psi) were observed in the laboratory in several pre-buckling and post-buckling states. Use of photographic methods for the measurement of the radial and tangential displacements of points marked along the meridians of the shells shows a region of small but very definite outward radial displacements adjacent to the main buckling dimple. Furthermore, the displacements observed were symmetric about the polar axis.

The experimental buckling pressures observed for the four shells tend to indicate that the critical pressure calculated according to the linear theory may be the correct one, i.e., the buckling pressures varied from about half to over three quarters of the linear buckling load.

CHAPTER I

INTRODUCTION

The rapidly advancing technology in the world today is making ever increasing demands upon the materials and structures in use and upon the ingenuity of the engineer to make more efficient use of the material at his disposal. Members that previously served only in nonstructural capacities are being asked to perform as load carrying members as well. In addition, severe weight and strength demands are being placed upon the structures so that it is becoming increasingly necessary to be able to predict accurately the load carrying capabilities of the members in order that the most efficient use can be made of the material used.

Some engineering structures subjected to specific types of loading display a buckling, or instability, phenomenon. The structure is able to withstand loads up to a certain critical load while deflecting only a small amount. As the critical, or Euler load is approached the structure becomes very sensitive to the addition of any further load. If the structure undergoes a large deflection when the critical load is applied, it is termed unstable at (or above) this load and the structure is said to have buckled.

The uniformly thick spherical shell is a structure which is generally accepted to exhibit such a phenomenon under certain types of loading—uniform external pressure, for instance. The study of this buckling problem has quite a long history dating back to the dissertation

of R. Zoelly[43] in 1915 and to an article by E. Schwerin[29] in 1922. A general solution which includes the effect of unsymmetrical buckling was advanced by A. van der Neut in his dissertation[36] published in 1932. An outline of the solution of the axisymmetric linear buckling problem for the case of a complete sphere under uniform external pressure, which turns out to be an eigenvalue problem, is given by Timoshenko.[35]

That the critical buckling load predicted by the linear theory is not approached experimentally has prompted investigators to pursue the solution of the nonlinear problem. In addition much work has been focused upon the buckling of small sectors of a spherical shell (often called a spherical cap) and also upon buckling under different loading conditions.

In order to reconcile the discrepancy between the theory and experience, von Kármán and his co-worker Tsien[38] cast aside the classical theory and proposed a new criterion for buckling—that of the "minimum buckling load." This concept says in essence that the shell, upon reaching the load at which there is a buckled equilibrium configuration available, will "jump" from the unbuckled to this buckled configuration and never reach the Euler load. These authors applied their new theory to the buckling of a thin spherical cap and obtained a minimum buckling load solution which conformed closely to experimental results. In a subsequent paper von Kármán, Dunn, and Tsien[37] pointed out that the energy needed to jump from the unbuckled to the buckled configuration may possibly be furnished by vibrations and random disturbances in the sur-

roundings. Initial imperfections in the shell are also cited as possible contributors to the unexpectedly low experimental buckling loads.

The results of von Kármán and Tsien[38] are largely refuted by Friedrichs[12] is a paper published in, ironically enough, the Theodore von Kármán Anniversary Volume. Friedrichs by the use of an asymptotic "boundary layer" technique shows that an assumption made by von Kármán and Tsien is sufficient to cause their results to be in error by a factor of two. He further points out that the potential energy of a shell which buckled at the Kármán-Tsien "minimum buckling load" is greater than that of unbuckled shell and mentions that, "It is hard to understand why the shell should leave the stable unbuckled state, jump to a state with a higher potential energy and stay there." In this light he proposes an "intermediate" buckling load which is the smallest load for which the potential energy of the buckled shell is less than that of the unbuckled shell. Friedrichs uses the Ritz method of obtaining numerical results and notes that the use of this method is questionable for problems such as this.

Tsien, in a paper[33] which followed that of Friedrichs closely, proposed a similar "lowest energy level" criterion which says that, subject to equilibrium of the external forces and internal stresses and subject to any geometric or loading constraints, buckling is most likely to occur at the load for which the potential energy of the unbuckled and the buckled states is the same. This theory agreed quite well with the experimental data available.

Then, Tsien in a short note[34] reverses himself and returns to the "lower buckling load" theory and states that this is surely the proper criterion on the grounds that the energy difference between unbuckled and buckled states is so nearly the same for the two criteria as to be negligible.

A sizable portion of the recent work done in the field of spherical shell buckling has been done by Eric Reissner and by those using the equations derived by him as a basis for their investigations. Reissner's first formulation[25] of the shallow spherical shell problem consists of a pair of fourth order linear differential equations which, he says, can be applied to nonshallow shells providing the resulting stresses are restricted to a shallow portion of the sphere. Small deflections are assumed. In a sequel[26] he shows that the fourth order equations can be reduced to second order equations and then solves these equations for the rotationally symmetric cases of the spherical cap with no edge restraint subjected to a point load at the apex and to a uniform load distributed over a small sector of the cap and of the cap with edge restraint carrying a point load at the apex.

Application of these small deflection equations of Reissner was extended by Ashwell[2] to describe a large segment of the spherical shell subjected to a point load at its apex. The load-deflection curve obtained agrees well with experiments. Considered also is the buckling of a thin cap under a central point load.

A more general theory involving the finite deflections of a thin shell of revolution was developed by Reissner[27] a short time later. The equations are linearized to give a small but finite deflection theory, and some observations are made concerning a few very limited specializations of the theory. A slightly different treatment is applied to the same basic equations in a subsequent paper;[28] two nonlinear ordinary differential equations for the small finite deflections of a shallow spherical shell of uniform thickness result. It is these equations which have received considerable attention.

A power series solution of these equations and a perturbation solution were first advanced by Simons[30] and Archer[1] respectively. The availability of the high speed digital computer made it possible for Weinitschke[41] to obtain more accurate results using the power series approach first used on the problem by Simons. A second power series solution was published in a paper by Weinitschke[42] in which he established the validity of the solution by showing the convergence of the series. Budiansky[5] tried a different approach by transforming the differential equations into integral equations and then solving the integral equations using an iterative procedure on the digital computer to obtain numerical results. Thurston[32] used a strictly numerical iteration procedure to solve Reissner's equations for both an upper and a lower buckling pressure. The critical loads obtained in these papers do not agree well with experiments (except perhaps in a very narrow range of a geometrical parameter); however, the results of Weinitschke and Budiansky agree re-

markably well with each other, as they pointed out in a recent paper.[6]

Other investigations have considered a variety of loading and boundary conditions. An early work by Biezeno,[3,4] gives the solution to a nonlinear problem of a simply supported spherical cap subjected to a central point load. Chien and Hu[8] studied the behavior of a thin spherical cap under a symmetrical (circular) line load and under a uniform edge moment and found critical loads smaller than those observed in experiments. The two nonlinear differential equations of Chien[7] are used by Reiss, Greenberg, and Keller[24] and by Keller and Reiss[17] to study the case of the spherical cap with a fixed boundary subjected to a uniform external pressure. Power series and finite difference solutions respectively were used. Murray and Wright[21] used a combination of a power series and a step-by-step integration in obtaining a solution of the Kármán-Tsien equations for the case of a fixed boundary and pressure loading. Unsymmetric deformations for this case are considered by Grigolyuk[13] who indicates the method of solution but gets no usable results.

Several investigators, viz. Reiss,[23] von Willich,[39] Nash and Modeer,[22] and Wedellsborg,[40] have proposed approximate solutions which require less computational effort than do the more exact analyses and yet give satisfactory values for the buckling loads.

In spite of the fact that a rather large amount of theoretical work has been reported in the literature, a relatively small amount of experimental results appears. The experimental results most often used for comparison with theoretical results are those reported by Kaplan and

Fung in an NACA Technical Note.[16] Buckling pressures for twenty-three magnesium alloy spherical caps clamped on the boundary are given. Oil and air were used as loading media in order to approximate a constant volume and a constant pressure characteristic respectively. A theoretical analysis of the problem is also included.

Experiments performed by Klöppel and Jungbluth[18] on nonshallow shells showed an unsymmetric buckling mode with the buckle forming near the clamped boundary. This behavior was attributed to initial stress and thickness imperfections which were quite evident near the boundary. J.M.T. Thompson, in a recent paper,[31] presents results of experiments performed using two polyvinyl chloride shells and correlates these results with the theoretical behavior of an initially imperfect shell. Limited results of experiments performed by E. E. Sechler and W. Bollay and by L. G. Dunn and H. B. Crockett are reported by von Kármán and Tsien[38] and by Tsien[33] respectively.

So far, the stability of a specific structural configuration, the thin spherical shell, has been considered. Nonetheless, a general nonlinear theory for the buckling and post-buckling behavior of structures (assuming small finite deflections) has been formulated by Koiter.[20] This analysis is essentially a perturbation scheme which applies equally well to plates, shells, etc. Application of this theory to the behavior of a reinforced cylindrical shell subjected to an axial load has been made by Koiter.[19]

The present investigation seeks to apply a similar perturbation scheme to a complete spherical shell under a uniform external pressure. Owing to the complexity of the calculations only the second perturbation coefficients have been calculated; consequently, the results obtained are applicable only in the immediate neighborhood of the classical buckling load and give no indication of a Kármán-Tsien "lower buckling load."

Also undertaken in the course of the present study was an experimental program designed more to determine the shape of the buckling mode than to obtain the precise buckling pressures for the different shells. Since only four experimental specimens were tested, conclusions concerning buckling loads are tentative.

CHAPTER II

GENERAL THEORY

In the theoretical portion of this investigation we seek to establish the stability or instability of the equilibrium configurations adjacent to the unbuckled state of a complete thin spherical shell. The results obtained will be valid only in the neighborhood of the Euler load. As a start toward our goal we assume that the potential energy, i.e., the difference between the energy of the buckled state and that of the unbuckled state, is of the form:

$$\mathcal{V}(u,\lambda) \equiv V_2(u) + \lambda V_2^{\lambda}(u) + V_3(u) + V_4(u) \qquad (2\text{-}1)$$

where:

u = aggregate of all displacements from the unbuckled state

λ = load parameter

$\mathcal{V}$ = potential energy (a function of u and λ)

$V_n(u)$ = aggregate of all terms of nth order in the deflections u and their derivatives

$V_2^{\lambda}(u)$ = aggregate of the terms quadratic in u and its derivatives which have the load parameter λ as a coefficient.

Use of a linear stress-strain law and expressions for the strains that are quadratic in the displacements will indeed produce this form for the potential energy provided the third and higher order terms which have

the load parameter λ as a coefficient can be neglected.

Expansions of the polynomials V_n and V_2^{λ} take the form:

$$V_n(a+b) \equiv V_n(a) + V_{n-1,1}(a,b) + V_{n-2,2}(a,b) + \cdots + V_{1,n-1}(a,b) + V_n(b) \tag{2-2}$$

$$V_2^{\lambda}(a+b) \equiv V_2^{\lambda}(a) + V_{11}^{\lambda}(a,b) + V_2^{\lambda}(b) \tag{2-3}$$

Here $V_{ij}(a,b)$, etc., represent the polynomials which are of order i in a and its derivatives and of order j in b and its derivatives. Expansions for $V_n(a+b+c)$, etc., can be similarly represented.

With this notation at our disposal we can now proceed to apply our criteria for determining the equilibrium configurations of the shell; this will be done in two parts. Once equilibrium is established the stability, or instability of the equilibrium can then be determined readily (as will be seen later).

For the first part of our problem we require that the potential energy be stationary in the buckled state. Thus, the variation of the potential energy with respect to the displacements u must vanish. This condition takes the form:

$$\delta_u \mathcal{V}(u,\lambda) = V_{11}(u,\eta) + \lambda V_{11}^{\lambda}(u,\eta) + V_{21}(u,\eta) + V_{31}(u,\eta) = 0 \quad \text{for all } \eta \tag{2-4}$$

This set of equations represents the nonlinear differential equations for determining the buckled state associated with a given load. These can be reduced to linear differential equations by using a perturbation analysis.

That is, we assume that the displacements are analytic in the neighborhood of the unbuckled state so that they may be represented by a Taylor series with a finite circle of convergence. If ϵ is used as the expansion, or perturbation parameter, and x is the independent variable, the Taylor series takes the form:

$$u(x,\epsilon) = \epsilon u_1(x) + \epsilon^2 u_2(x) + \epsilon^3 u_3(x) + \cdots \qquad (2\text{-}5)$$

where:

$$V_{11}^{\lambda}(u_1,u_i) = 0 \qquad (i = 2,3,4,\cdots)*$$

The functions u_i, for i = 1,2,3, etc., are at this point undetermined. It would be expected that this expansion should start with a term u_0, but since we require that the deflections vanish for a vanishing perturbation parameter ϵ, this term must be identically zero. Substituting this expansion (2-5) into the potential energy expression (2-1) gives:

$$\begin{aligned}
\mathcal{V}(\epsilon,\lambda) = {} & \epsilon^2\{V_2(u_1) + \lambda V_2^{\lambda}(u_1)\} \\
& + \epsilon^3\{V_{11}(u_1,u_2) + \lambda V_{11}^{\lambda}(u_1,u_2) + V_3(u_1)\} \\
& + \epsilon^4\{V_{11}(u_1,u_3) + \lambda V_{11}^{\lambda}(u_1,u_3) + V_2(u_2) \\
& \quad + \lambda V_2^{\lambda}(u_2) + V_{21}(u_1,u_2) + V_4(u_1)\} \\
& + \epsilon^5\{V_{11}(u_1,u_4) + \lambda V_{11}^{\lambda}(u_1,u_4) + V_{11}(u_2,u_3) \\
& \quad + \lambda V_{11}^{\lambda}(u_2,u_3) + V_{21}(u_1,u_3) + V_{12}(u_1,u_2) \\
& \quad + V_{31}(u_1,u_2)\} + \cdots
\end{aligned} \qquad (2\text{-}6)$$

*This specification together with an arbitrary normalizing condition for u_1, is necessary and sufficient for defining ϵ uniquely.

We are now in a position to apply the requirement for the equilibrium of the buckled configuration that the potential energy must be stationary with respect to the perturbation parameter ϵ for a given constant value of the load parameter λ. Thus, the derivative of the potential energy with respect to ϵ must vanish for a constant λ. This condition is:

$$\left.\frac{d\mathcal{V}}{d\epsilon}\right|_{\lambda=\text{const.}} = 0 \tag{2-7}$$

Now, if the load parameter λ is analytic in the neighborhood of the buckling load, it can be represented by a Taylor series with a finite circle of convergence. We thus expand λ in powers of the perturbation parameter ϵ, the same parameter used in the expansion for the deflections:

$$\lambda(\epsilon) = \lambda_0 + \epsilon\lambda_1 + \epsilon^2\lambda_2 + \epsilon^3\lambda_3 + \cdots \tag{2-8}$$

Applying condition (2-7) to the expression (2-6) for the potential energy and then substituting the expansion (2-8) gives the condition:

$$\begin{aligned}
\left.\frac{d\mathcal{V}}{d\epsilon}\right|_{\lambda=\text{const.}} = {} & \epsilon\{2V_2(u_1) + 2\lambda_0 V_2^{\lambda}(u_1)\} \\
& + \epsilon^2\{3V_{11}(u_1,u_2) + 3\lambda_0 V_{11}^{\lambda}(u_1,u_2) + 3V_3(u_1) \\
& \quad + 2\lambda_1 V_2^{\lambda}(u_1)\} \\
& + \epsilon^3\{4V_{11}(u_1,u_3) + 4\lambda_0 V_{11}^{\lambda}(u_1,u_3) + 4V_2(u_2) \\
& \quad + 4\lambda_0 V_2^{\lambda}(u_2) + 4V_{21}(u_1,u_2) + 4V_4(u_1) \\
& \quad + 3\lambda_1 V_{11}^{\lambda}(u_1,u_2) + 2\lambda_2 V_2^{\lambda}(u_1)\} \\
& + \epsilon^4\{5V_{11}(u_1,u_4) + 5\lambda_0 V_{11}^{\lambda}(u_1,u_4) + 5V_{11}(u_2,u_3) \\
& \quad + 5\lambda_0 V_{11}^{\lambda}(u_2,u_3) + 5V_{21}(u_1,u_3) + 5V_{12}(u_1,u_2) \\
& \quad + 5V_{31}(u_1,u_2) + 4\lambda_1 V_2^{\lambda}(u_2) + 4\lambda_1 V_{11}^{\lambda}(u_1,u_3) \\
& \quad + 3\lambda_2 V_{11}^{\lambda}(u_1,u_2) + 2\lambda_3 V_2^{\lambda}(u_1)\} \\
& + \cdots = 0 \qquad \text{for all } \epsilon
\end{aligned} \tag{2-9}$$

Substitution of the perturbation expansions (2-5) and (2-8) into the equilibrium condition (2-4) yields:

$$\begin{aligned}
&\epsilon\{V_{11}(u_1,\eta) + \lambda_0 V^{\lambda}_{11}(u_1,\eta)\} \\
&+ \epsilon^2\{V_{11}(u_2,\eta) + \lambda_0 V^{\lambda}_{11}(u_2,\eta) + \lambda_1 V^{\lambda}_{11}(u_1,\eta) + V_{21}(u_1,\eta)\} \\
&+ \epsilon^3\{V_{11}(u_3,\eta) + \lambda_0 V^{\lambda}_{11}(u_3,\eta) + \lambda_1 V^{\lambda}_{11}(u_2,\eta) + \lambda_2 V^{\lambda}_{11}(u_1,\eta) \\
&\qquad + V_{111}(u_1,u_2,\eta) + V_{31}(u_1,\eta)\} \\
&+ \epsilon^4\{V_{11}(u_4,\eta) + \lambda_0 V^{\lambda}_{11}(u_4,\eta) + \lambda_1 V^{\lambda}_{11}(u_3,\eta) + \lambda_2 V^{\lambda}_{11}(u_2,\eta) \\
&\qquad + \lambda_3 V^{\lambda}_{11}(u_1,\eta) + V_{21}(u_2,\eta) + V_{111}(u_1,u_3,\eta) + V_{211}(u_1,u_2,\eta)\} \\
&+ \cdots = 0 \qquad \text{for all } \eta \text{ and all } \epsilon \qquad (2\text{-}10)
\end{aligned}$$

Since Eqs. (2.9) and (2-10) are valid for all values of ϵ, a necessary and sufficient condition for their satisfaction is the vanishing of the coefficients of the various powers of ϵ individually.

The coefficients from Eq. (2-10) are the linear differential equations which now describe our problem. For instance, the terms that are first order in ϵ, i.e., have ϵ^1 as a coefficient, constitute the linear eigenvalue problem for the buckling mode u_1 and buckling load λ_0 of a spherical shell. The solution of this problem is now well known and is described by Timoshenko.[35] The expressions in Eq. (2-10) which are quadratic, cubic, etc., in the perturbation parameter ϵ are in turn the linear nonhomogeneous differential equations for the perturbation functions u_2, u_3, etc.

Since Eq. (2-9) covers the variation for which ϵ, and only ϵ, changes (that is, tangent to the path), the whole space of variations

is filled if, in addition, all variations η which are orthogonal to u_1 are considered.* In other words, all variations η satisfying:

$$V^{\lambda}_{11}(u_1,\eta) = 0 \tag{2-11}$$

are to be considered. If we thus impose these side conditions on our solutions by using the Lagrangian multipliers $\mu_i (i = 0,1,2,\cdots)$, our differential equations become:

$$V_{11}(u_1,\eta) + \lambda_0 V^{\lambda}_{11}(u_1,\eta) + \mu_0 V^{\lambda}_{11}(u_1,\eta) = 0 \tag{2-12}$$

$$V_{11}(u_2,\eta) + \lambda_0 V^{\lambda}_{11}(u_2,\eta) + \lambda_1 V^{\lambda}_{11}(u_1,\eta) + V_{21}(u_1,\eta) + \mu_1 V^{\lambda}_{11}(u_1,\eta) = 0 \tag{2-13}$$

$$\begin{aligned} &V_{11}(u_3,\eta) + \lambda_0 V^{\lambda}_{11}(u_3,\eta) + \lambda_1 V^{\lambda}_{11}(u_2,\eta) + \lambda_2 V^{\lambda}_{11}(u_1,\eta) \\ &\quad + V_{111}(u_1,u_2,\eta) + V_{31}(u_1,\eta) + \mu_2 V^{\lambda}_{11}(u_1,\eta) = 0 \end{aligned} \tag{2-14}$$

$$\begin{aligned} &V_{11}(u_4,\eta) + \lambda_0 V^{\lambda}_{11}(u_4,\eta) + \lambda_1 V^{\lambda}_{11}(u_3,\eta) + \lambda_2 V^{\lambda}_{11}(u_2,\eta) \\ &\quad + \lambda_3 V^{\lambda}_{11}(u_1,\eta) + V_{21}(u_2,\eta) + V_{111}(u_1,u_3,\eta) \\ &\quad + V_{211}(u_1,u_2,\eta) + \mu_3 V^{\lambda}_{11}(u_1,\eta) = 0 \end{aligned} \tag{2-15}$$

These Eqs. (2-12) through (2-15) are now valid for an arbitrary variation η.

The vanishing of the coefficients of the various powers of ϵ in Eq. (2-9) yields the following set of equations:

---

*Provided that the path itself is not orthogonal to u_1, in which case the perturbation procedure is known to diverge anyway.

$$V_2(u_1) + \lambda_0 V_2^{\lambda}(u_1) = 0 \tag{2-16}$$

$$3V_{11}(u_1,u_2) + 3\lambda_0 V_{11}^{\lambda}(u_1,u_2) + 3V_3(u_1) + 2\lambda_1 V_2^{\lambda}(u_1) = 0 \tag{2-17}$$

$$4V_{11}(u_1,u_3) + 4\lambda_0 V_{11}^{\lambda}(u_1,u_3) + 4V_2(u_2) + 4\lambda_0 V_2^{\lambda}(u_2) + 4V_{21}(u_1,u_2) + 4V_4(u_1) + 3\lambda_1 V_{11}^{\lambda}(u_1,u_2) + 2\lambda_2 V_2^{\lambda}(u_1) = 0 \tag{2-18}$$

$$5V_{11}(u_1,u_4) + 5\lambda_0 V_{11}^{\lambda}(u_1,u_4) + 5V_{11}(u_2,u_3) + 5\lambda_0 V_{11}^{\lambda}(u_2,u_3) + 5V_{21}(u_1,u_3) + 5V_{12}(u_1,u_2) + 5V_{31}(u_1,u_2) + 4\lambda_1 V_2^{\lambda}(u_2) + 4\lambda_1 V_{11}^{\lambda}(u_1,u_3) + 3\lambda_2 V_{11}^{\lambda}(u_1,u_2) + 2\lambda_3 V_2^{\lambda}(u_1) = 0 \tag{2-19}$$

Our variational problem thus reduces to the solution of the linear differential Eqs. (2-12) through (2-15) subject to the conditions (2-16) through (2-19). This system of equations can be simplified considerably.

At this point we prove an identity and state four others (without proof) which will be necessary to carry out a detailed analysis of the development which follows. Let us show that:

$$V_{11}(a,a) \equiv 2V_2(a) \tag{2-20}$$

Starting with $V_2(a)$:

$$V_2(a) \equiv V_2\left(\frac{a}{2} + \frac{a}{2}\right) = \frac{1}{2} V_2(a) + \frac{1}{4} V_{11}(a,a) \tag{2-21}$$

$$\therefore \quad V_{11}(a,a) \equiv 2V_2(a) \qquad \text{Q.E.D.} \tag{2-20}$$

Similarly, it can be shown:

$$V_{11}^{\lambda}(a,a) \equiv 2V_2^{\lambda}(a) \tag{2-22}$$

$$V_{111}(a,b,a) \equiv 2V_{21}(a,b) \tag{2-23}$$

$$V_{21}(a,a) \equiv 3V_3(a) \tag{2-24}$$

$$V_{31}(a,a) \equiv 4V_4(a) \tag{2-25}$$

Now, we proceed with the simplification of our system of equations. Since η is arbitrary, let $\eta = u_1$ in Eq. (2-12) and then apply the identity (2-21). The result is:

$$V_2(u_1) + \lambda_o V_2^{\lambda}(u_1) + \mu_o V_2^{\lambda}(u_1) = 0 \tag{2-26}$$

Simultaneous solution of this Eq. (2-26) with Eq. (2-16) implies:

$$\mu_o = 0 \tag{2-27}$$

Thus, upon applying the condition (2-27) to Eq. (2-12) the variational equation for determining the linear buckling mode u_1 and the corresponding buckling λ_o becomes, as is well-known:

$$V_{11}(u_1,\eta) + \lambda_o V_{11}^{\lambda}(u_1,\eta) = 0 \tag{2-28}$$

A similar procedure using Eq. (2-13) with $\eta = u_1$, (2-17), and (2-28) with $\eta = u_2$, yields the simplifying condition:

$$\mu_1 = 0 \tag{2-29}$$

and the differential Eq. (2-13) for obtaining u_2 becomes:

$$V_{11}(u_2,\eta) + \lambda_o V_{11}^{\lambda}(u_2,\eta) + \lambda_1 V_{11}^{\lambda}(u_1,\eta) + V_{21}(u_1,\eta) = 0 \tag{2-30}$$

Solving Eqs. (2-17) and (2-28) with $\eta = u_2$ simultaneously gives the result:

$$\lambda_1 = -\frac{3}{2}\frac{V_3(u_1)}{V_2^{\lambda}(u_1)} \tag{2-31}$$

A similar scheme—using Eqs. (2-14) with $\eta = u_1$, (2-18), (2-28) with $\eta = u_3$, and (2-30) with $\eta = u_2$—implies that:

$$\mu_2 = 0 \tag{2-32}$$

Also, the use of Eqs. (2-14) with $\eta = u_1$ and (2-28) with $\eta = u_3$ and conditions (2-11) with $\eta = u_2$ and (2-32) yields the expression for λ_2:

$$\lambda_2 = -\frac{V_{21}(u_1,u_2) + 2V_4(u_1)}{V_2^{\lambda}(u_1)} \tag{2-33}$$

Although it will not be used in the course of the present investigation, an expression for the third load perturbation coefficient λ_3 can be derived using techniques similar to, but somewhat more involved than those used above. This expression is:

$$\lambda_3 = -\frac{5V_{12}(u_1,u_2) + 5V_{31}(u_1,u_2) + 4\lambda_1 V_2^{\lambda}(u_2)}{2V_2^{\lambda}(u_1)} \tag{2-34}$$

Note that this expression is not dependent upon the third deflection perturbation function u_3.

Once we have calculated values for λ_1 and λ_2 we can determine from them whether the equilibrium configurations adjacent to the unbuckled

state are stable or unstable. Recalling that the load parameter has been expanded so:

$$\lambda(\epsilon) = \lambda_0 + \epsilon\lambda_1 + \epsilon^2\lambda_2 + \epsilon^3\lambda_3 + \cdots \qquad (2\text{-}8 \text{ bis})$$

we see that the first derivative of λ with respect to the perturbation parameter ϵ (which indicates the amplitude of buckling) for a vanishing ϵ gives the slope of the load-deflection curve at the point of buckling. This value, namely λ_1, if it is other than zero indicates that there are adjacent equilibrium states for loads smaller than the Euler load and thus the equilibrium is unstable. The algebraic sign of λ_1 is inconsequential since the sign of ϵ is arbitrary.

In the case that the perturbation coefficient λ_1 is zero it is necessary to investigate the value of the next perturbation coefficient λ_2 in order to establish the stability or instability of the structure under study. The second derivative of λ with respect to ϵ for vanishing ϵ is $2\lambda_2$ and its algebraic sign indicates whether the load-deflection curve is concave upward or concave downward. Should λ_2 be positive the curve is concave upward for a vanishing amplitude ϵ and adjacent equilibrium configurations exist only at loads greater than the Euler load. The equilibrium is thus stable. Conversely, if λ_2 is negative, the load-deflection curve is concave downward at $\epsilon = 0$, adjacent equilibrium configurations exist for loads less than the Euler load, and the equilibrium is thus unstable. Thus, stability, or instability, in the neighborhood of the buckling load reduces to the evaluation of the load perturbation

coefficients λ_1 and λ_2.

A nonlinear analysis of this type for the problem of the buckling of an axially loaded column would not be prompted since the buckling load predicted by the linear theory is closely approached in experiments. Such agreement, however, is not encountered in the case of the buckling of a spherical shell subjected to a uniform external pressure. In practice, spherical shells buckle at loads somewhat below values calculated using the linear theory, and a nonlinear analysis is prompted to try to explain the inadequacy of the linear theory. An instability at the buckling load as indicated by the nonlinear analysis would lend credibility to the belief that the buckling of spherical shells is very sensitive to initial imperfections and to random disturbances.

CHAPTER III

APPLICATION TO SPHERICAL SHELLS

In the section on general theory little was said concerning the thin spherical shell which is the object of this investigation—the general theory is applicable to structures in general. In this section the theory is applied to a complete, uniformly thick, spherical shell which is acted upon by a uniform external load and which is restricted to axially symmetric deflections.

Our first job is to determine the buckling energy of the shell. From this we shall be able to apply the general theory in order to obtain the form of the load parameter λ and consequently determine the shell's stability or instability as the case may be. It will be shown that the shell is unstable in the neighborhood of the linear buckling load λ_o.

The Cartesian coordinates x^{i*} of a point may be described in terms of the spherical polar coordinates r (the radial distance from the origin), α (the polar angle), and ϕ (the longitude):

$$\begin{aligned} x^1 &= r \sin\alpha \cos\phi \\ x^2 &= r \sin\alpha \sin\phi \\ x^3 &= r \cos\alpha \end{aligned} \qquad (3\text{-}1)$$

*Unless otherwise noted, superscripts may have the values 1,2,3, and a repeated superscript indicates summation over these values.

The metric tensor $g_{\alpha\beta}$ is (letting $y^i = (r,\alpha,\phi)$):

$$g_{\alpha\beta} \equiv \frac{\partial x^i}{\partial y^\alpha}\frac{\partial x^i}{\partial y^\beta} \tag{3-2}$$

$$g_{\alpha\beta} = \begin{bmatrix} 1 & 0 & 0 \\ 0 & r^2 & 0 \\ 0 & 0 & r^2\sin^2\alpha \end{bmatrix} \tag{3-3}$$

If we assume axial symmetry and let the point be displaced an amount w radially toward the origin and an amount v tangentially in the positive α direction, the point's Cartesian coordinates $\bar{x}^i$ can be expressed:

$$\begin{aligned} \bar{x}^1 &= [(r-w)\sin\alpha + v\cos\alpha]\cos\phi \\ \bar{x}^2 &= [(r-w)\sin\alpha + v\cos\alpha]\sin\phi \\ \bar{x}^3 &= (r-w)\cos\alpha - v\sin\alpha \end{aligned} \tag{3-4}$$

The components of the metric tensor here are:

$$G_{\alpha\beta} \equiv \frac{\partial \bar{x}^i}{\partial y^\alpha}\frac{\partial \bar{x}^i}{\partial y^\beta} \tag{3-5}$$

$$\begin{aligned} G_{rr} &= (1-w_{,r})^2 + v_{,r}^2 \\ G_{r\alpha} &= v_{,r}(r-w+v_{,\alpha}) - (v+w_{,\alpha})(1-w_{,r}) \\ G_{\alpha\alpha} &= (r-w+v_{,\alpha})^2 + (v+w_{,\alpha})^2 \\ G_{\phi\phi} &= [(r-w)\sin\alpha + v\cos\alpha]^2 \\ G_{r\phi} &= G_{\alpha\phi} = 0 \end{aligned} \tag{3-6}$$

where the subscripted comma denotes partial differentiation with respect to the variable which follows it. Note that due to the restriction of axial symmetry imposed, the displacements v and w are functions of r and α only. The covariant and physical components of strain respectively are defined by:

$$\epsilon_{\alpha\beta} \equiv \frac{1}{2}(G_{\alpha\beta}-g_{\alpha\beta}) \tag{3-7}$$

$$\epsilon^{P}_{\alpha\beta} \equiv \frac{\epsilon_{\alpha\beta}}{\sqrt{g_{\alpha\alpha}g_{\beta\beta}}} \qquad \text{(no sum on } \alpha \text{ and } \beta) \tag{3-8}$$

Then, the physical components of strain are (since we shall be dealing with the physical components only, we may drop the "P" notation without danger of confusion):

$$\begin{aligned}
\epsilon_{rr} &= -w_{,r} + \frac{1}{2}(v^2_{,r}+w^2_{,r}) \\
\epsilon_{r\alpha} &= \frac{1}{r}[v_{,r}(r-w+v_{,\alpha}) - (v+w_{,\alpha})(1-w_{,r})] \\
\epsilon_{\alpha\alpha} &= \frac{1}{r}(v_{,\alpha}-w) + \frac{1}{2r^2}[(v_{,\alpha}-w)^2 + (v+w_{,\alpha})^2] \\
\epsilon_{\phi\phi} &= \frac{1}{r}(v\cot\alpha-w) + \frac{1}{2r^2}(v\cot\alpha-w)^2 \\
\epsilon_{r\phi} &= \epsilon_{\alpha\phi} = 0
\end{aligned} \tag{3-9}$$

Let us now make a change of variables and reduce our problem to a one-dimensional problem by making assumptions invoking the thinness of the shell. The change of variables is:

$$r = R - z \tag{3-10}$$

where

R = radius of the midsurface of the undeformed shell

z = distance from R (toward the origin)

Physical considerations indicate that the strains ϵ_{rr} and $\epsilon_{r\alpha}$ be small for a thin shell; therefore, we make the substitutions:

$$v \to v - \frac{z}{R}(v+w')$$
$$w \to w \qquad (3\text{-}11)$$

where v and w are now displacements of a point of the midsurface and are functions of α alone. (Primes denote differentiation with respect to α.) These substitutions cause the linear terms of ϵ_{rr} and $\epsilon_{r\alpha}$ to vanish, i.e., the major terms vanish, and the remaining terms are of higher order. Therefore, we assume:

$$\epsilon_{rr} = \epsilon_{r\alpha} = 0 \qquad (3\text{-}12)$$

Use of the expansions:

$$\frac{1}{R-z} \equiv \frac{1}{R(1-\frac{z}{R})} = \frac{1}{R}\left[1 + \frac{z}{R} + (\frac{z}{R})^2 + (\frac{z}{R})^3 + \cdots\right]$$
$$\frac{1}{(R-z)^2} \equiv \frac{1}{R^2(1-\frac{z}{R})^2} = \frac{1}{R^2}\left[1 + 2\frac{z}{R} + 3(\frac{z}{R})^2 + 4(\frac{z}{R})^3 + \cdots\right] \qquad (3\text{-}13)$$

and the substitutions (3-11) produces the remaining strain components:

$$\epsilon_{\alpha\alpha} = \frac{1}{R}(v'-w) + \frac{1}{2R^2}[(v'-w)^2 + (v+w')^2]$$

$$- \frac{z}{R}\left[\frac{1}{R^2}(w+w'')(R+v'-w)\right]$$

$$- \left(\frac{z}{R}\right)^2\left[\frac{1}{R^2}(w+w'')(R+v' - \frac{3}{2}w - \frac{1}{2}w'')\right]$$

$$- \left(\frac{z}{R}\right)^3\left[\frac{1}{R^2}(w+w'')(R+v'-2w-w'')\right]$$

$$- \cdots \qquad (3\text{-}14)$$

$$\epsilon_{\phi\phi} = \frac{1}{R}(v\cot\alpha - w) + \frac{1}{2R^2}(v\cot\alpha - w)^2$$

$$- \left(\frac{z}{R}\right)\left[\frac{1}{R^2}(w'\cot\alpha + w)(R + v\cot\alpha - w)\right]$$

$$- \left(\frac{z}{R}\right)^2\left[\frac{1}{R^2}(w'\cot\alpha + w)(R + v\cot\alpha - \frac{3}{2}w - \frac{1}{2}w'\cot\alpha)\right]$$

$$- \left(\frac{z}{R}\right)^3\left[\frac{1}{R^2}(w'\cot\alpha + w)(R + v\cot\alpha - 2w - w'\cot\alpha)\right]$$

$$- \cdots \qquad (3\text{-}15)$$

$$\epsilon_{r\phi} = \epsilon_{\alpha\phi} = 0 \qquad (3\text{-}16)$$

Making simplifying approximations of the type used by Donnell[10] and by Friedrichs in his asymptotic treatment[12] yields the strain components $\epsilon_{\alpha\alpha}$ and $\epsilon_{\phi\phi}$ in the form:

$$\epsilon_{\alpha\alpha} \cong \frac{1}{R}(v'-w) + \frac{1}{2R^2}w'^2 - \left(\frac{z}{R}\right)\frac{1}{R}w'' \qquad (3\text{-}17)$$

$$\epsilon_{\phi\phi} \cong \frac{1}{R}(v\cot\alpha - w) - \left(\frac{z}{R}\right)\frac{1}{R}w'\cot\alpha \qquad (3\text{-}18)$$

We are now in a position to calculate the strain energy of the shell. For our particular case the strain energy S can be shown to re-

duce to:

$$S = \int_V (\tau^o_{\alpha\alpha}\epsilon_{\alpha\alpha}+\tau^o_{\phi\phi}\epsilon_{\phi\phi})dV + \frac{E}{2(1-\nu^2)} \int_V (\epsilon^2_{\alpha\alpha}+\epsilon^2_{\phi\phi}+2\nu\epsilon_{\alpha\alpha}\epsilon_{\phi\phi})dV \quad (3\text{-}19)$$

Where E is Young's modulus, ν is Poisson's ratio, $\tau^o_{\alpha\alpha}$ and $\tau^o_{\phi\phi}$ are the stresses prior to buckling, dV is the volume increment, and the integral is taken over the volume of the shell. The initial stresses are:

$$\tau^o_{\alpha\alpha} = -\frac{pR}{2h} \quad (3\text{-}20)$$

$$\tau^o_{\phi\phi} = -\frac{pR}{2h} \quad (3\text{-}21)$$

Here:

p = uniform external pressure

h = shell thickness

If we substitute the expressions (3-17), (3-18), and (3-20), into (3-19), integrate over the thickness of the shell, and perform the indicated integrations by parts, the result is:

$$\begin{aligned} S = {} & p\int_A w dA + \frac{Eh}{2R^2(1-\nu^2)} \int_A \{[(v'-w)^2 \\ & + (v\cot\alpha - w)^2 + \frac{1}{R}(v'-w)w'^2 + \frac{1}{4R^2}w'^4 \\ & + 2\nu(v'-w)(v\cot\alpha - w) + \frac{\nu}{R}(v\cot\alpha - w)w'^2] \\ & + k[w''^2 + w'^2\cot^2\alpha + 2\nu w''w'\cot\alpha] \\ & - \frac{\lambda}{4}w'^2\}dA \end{aligned} \quad (3\text{-}22)$$

where dA is an element of shell area and the dimensional parameters k and λ are:

$$k = \frac{h^2}{12R^2} \tag{3-23}$$

$$\lambda = \frac{2pR(1-\nu^2)}{Eh} \tag{3-24}$$

Since the external work done during buckling is done under constant pressure conditions, the work, W, is:

$$W = p(V_o - V_f) \tag{3-25}$$

where:

V_o = initial volume

V_f = final volume

The initial volume is:

$$V_o = \frac{R^3}{3} \int_A dA \tag{3-26}$$

The final volume is:

$$V_f = \frac{1}{3} \int_A \vec{r} \cdot \vec{n} \, dA \tag{3-27}$$

where:

$\vec{r}$ = position vector

$\vec{n}$ = unit outer normal vector

Now,

$$\vec{n} \, dA = \frac{\partial \vec{r}}{\partial \alpha} \times \frac{\partial \vec{r}}{\partial \phi} \, d\alpha d\phi \tag{3-28}$$

Let the position vector be expressed by:

$$\vec{r} = x\vec{i} + y\vec{j} + z\vec{k} \tag{3-29}$$

where $\vec{i}$, $\vec{j}$, and $\vec{k}$ are base vectors and x, y, and z are the components of $\vec{r}$ in the directions of the respective base vectors. Further, let:

$$\begin{aligned} x &= [(R-w)\sin\alpha + v\cos\alpha]\cos\phi \\ y &= [(R-w)\sin\alpha + v\cos\alpha]\sin\phi \\ z &= (R-w)\cos\alpha - v\sin\alpha \end{aligned} \tag{3-30}$$

(Notice that it is here implied that the load is being applied at the midsurface of the shell rather than at the outer surface.) Carrying out the indicated manipulations and integrating by parts where indicated gives the final volume in the form:

$$\begin{aligned} V_f = \frac{1}{3}\int_A \{R - 3w + \frac{1}{R}[v^2+3w^2+v'v\cot\alpha+3vw'] \\ + \frac{1}{R^2}[v^3\cot\alpha - w^3 - 3vw'w - 3v'vw\cot\alpha]\}dA \end{aligned} \tag{3-31}$$

Thus, the work becomes:

$$\begin{aligned} W = p\int_A \{w - \frac{1}{R}[(w^2+vw') + \frac{1}{3}v(v'\cot\alpha+v)] \\ - \frac{1}{R^2}[-vw(v'\cot\alpha+w') + \frac{1}{3}(v^3\cot\alpha - w^3)]\}dA \end{aligned} \tag{3-32}$$

This result is applicable for a complete spherical shell, and for a segment of a shell providing the tangential displacement vanishes on the boundary.

The potential energy is defined as the difference between the strain energy of buckling and the work done during buckling. By observing the expressions for the strain energy (3-22) and the work done (3-32) one sees that the linear terms cancel with each other as the theorem of virtual work predicts. Finally, if we neglect the quadratic and cubic terms of the work with respect to the load term in the strain energy in order to be consistent with the simplifications made for Eqs. (3-17) and (3-18), the potential energy becomes:

$$\mathcal{V} = \frac{Eh}{2R^2(1-\nu^2)} \int_A \{[(v'-w)^2 + (v\cot\alpha - w)^2 + \frac{1}{R}(v'-w)w'^2 + \frac{1}{4R^2}w'^4 + 2\nu(v'-w)(v\cot\alpha - w) + \frac{\nu}{R}(v\cot\alpha - w)w'^2] + k[w''^2 + w'^2\cot^2\alpha + 2\nu w''w'\cot\alpha] - \frac{\lambda}{4}w'^2\}dA \qquad (3\text{-}33)$$

From this it can be seen that the polynomials of the previous section are:

$$V_2(u) = \frac{Eh}{2R^2(1-\nu^2)} \int_A \{[(v'-w)^2 + (v\cot\alpha - w)^2 + 2\nu(v'-w)(v\cot\alpha - w)] + k[w''^2 + w'^2\cot^2\alpha + 2\nu w''w'\cot\alpha]\}dA \qquad (3\text{-}34)$$

$$V_2^{\lambda}(u) = \frac{Eh}{2R^2(1-\nu^2)} \int_A \{-\frac{1}{4}w'^2\}dA \qquad (3\text{-}35)$$

$$V_3(u) = \frac{Eh}{2R^2(1-\nu^2)} \int_A \{\frac{1}{R}[(v'-w)w'^2 + \nu(v\cot\alpha - w)w'^2]\}dA \qquad (3\text{-}36)$$

$$V_4(u) = \frac{Eh}{2R^2(1-\nu^2)} \int_A \{\frac{1}{4R^2} w'^4\} dA \qquad (3\text{-}37)$$

It is now a simple matter to apply the theory developed in the previous section.

Taking the variations of the second order terms of the potential energy (3-33) with respect to v and w and then introducing v_1, w_1, and λ_o (for v, w, and λ) according to Eq. (2-28) gives the following two homogeneous linear differential equations:

$$v_1'' + v_1 \cot \alpha - (\nu + \cot^2\alpha) v_1 - (1+\nu) w_1' = 0 \qquad (3\text{-}38)$$

$$(1+\nu)[v_1' + v_1 \cot \alpha - 2w_1] + k[-w_1^{IV} - 2w_1''' \cot \alpha + (1+\nu+\cot^2\alpha) w_1'' - (2-\nu+\cot^2\alpha) w_1' \cot \alpha] - \frac{\lambda_o}{4} (w_1'' + w_1' \cot \alpha) = 0 \qquad (3\text{-}39)$$

The buckling mode for this eigenvalue problem is expressible in terms of one of the spherical harmonics $P_n(\cos \alpha)$ such that:

$$v_1 = A_n \frac{d}{d\alpha} [P_n(\cos \alpha)] \qquad (3\text{-}40)$$

$$w_1 = B_n P_n(\cos \alpha) \qquad (3\text{-}41)$$

Here n is an integer which designates the order of the spherical harmonic and A_n and B_n are constants associated with the given spherical harmonic. B_n is related to A_n by:

$$A_n = KB_n \qquad (3\text{-}42)$$

where:

$$K = -\frac{(1+\nu)}{n(n+1)-1+\nu} \qquad (3\text{-}43)$$

B_n is now an arbitrary amplitude constant which corresponds to the perturbation parameter, ϵ, of Chapter II. Therefore, it is convenient to let B_n assume the value one. Thus:

$$v_1 = K \frac{d}{d\alpha} [P_n(\cos \alpha)] \tag{3-44}$$

$$w_1 = P_n(\cos \alpha) \tag{3-45}$$

For a given value of n, the "classical" critical buckling load is calculated from:

$$\frac{\lambda_o}{4} = \frac{(1-\nu^2)\Gamma_n + k[\Gamma_n^3 + 2(2+\nu)\Gamma_n^2 + (1+\nu)(5+\nu)\Gamma_n + 2(1+\nu)^2]}{\Gamma_n^2 + (3+\nu)\Gamma_n + 2(1+\nu)} \tag{3-46}$$

where:

$$\Gamma_n = n(n+1) - 2 \tag{3-47}$$

By treating the load λ_o as a continuous function of Γ_n we can find the minimum value for the load by imposing the condition:

$$\frac{d\lambda_o}{d\Gamma_n} = 0 \tag{3-48}$$

This condition dictates the value of k for which the minimum load so calculated is valid, according to the relation:

$$k = \frac{(1-\nu^2)\Gamma_n^2 - 2(1+\nu)(1-\nu^2)}{\Gamma_n^4 + 2(3+\nu)\Gamma_n^3 + (13+10\nu+\nu^2)\Gamma_n^2 + 4(1+\nu)(3+\nu)\Gamma_n + 4(1+\nu)^2} \tag{3-49}$$

Inserting this value of k back into Eq. (3-46) gives the minimum critical buckling load, and simultaneous solution of this Eq. (3-49) with the

relation which defines k (3-23) yields the radius/thickness ratio of the shell.

This linear analysis, which has incorporated certain simplifications (see Eqs. (3-17), (3-18), and (3-33)), parallels the analysis given in greater detail by Timoshenko.[35]

The solution of the linear problem furnishes also the information necessary for determining the value of λ_1. The integral expressions $V_3(u_1)$ and $V_2^{\lambda}(u_1)$ are involved here as is evident from Eq. (2-31). Upon introducing expressions (3-44) and (3-45) for v_1 and w_1 and making a convenient change of variables:

$$x = \cos \alpha \tag{3-50}$$

one gets $V_3(u_1)$ in terms of Legendre polynomials. Then, use of Legendre's equation simplifies the result to:

$$V_3(u_1) = \frac{\pi Eh}{R(1-\nu^2)} \int_{-1}^{1} \{(1-x^2)P_n'^2[K(1-\nu)xP_n' - [Kn(n+1) + (1+\nu)]P_n]\}dx \tag{3-51}$$

where P_n now represents the Legendre polynomial of order n and primes denote differentiation with respect to x. Similarly, the integral expression for $V_2^{\lambda}(u_1)$ can be obtained, and the expression can be simplified to give:

$$V_2^{\lambda}(u_1) = -\frac{\pi Eh}{(1-\nu^2)} \left\{\frac{n(n+1)}{2(2n+1)}\right\} \tag{3-52}$$

The differential recurrence formulae, the expansion of $P_n'(x)$ in a series of Legendre polynomials, and the expressions for the integrals, $\int_{-1}^{1} P_n^2(x)dx$ and $\int_{-1}^{1} P_n'^2(x)dx$, are needed.[14,15] λ_1 is then easily obtained by use of Eq. (2-31).

Our next job is to solve Eq. (2-30) for the case of the spherical shell. The equations to be solved are obtained by taking the variations with respect to v and w of all but the fourth order term of the potential energy (3-33), introducing the perturbation expansions as indicated by Eqs. (2-5) and (2-8), and isolating the terms which are quadratic in ϵ. The two nonhomogeneous linear ordinary differential equations which result are:

$$v_2'' + v_2'\cot\alpha - (\nu+\cot^2\alpha)v_2 - (1+\nu)w_2' = -\frac{1}{R}\{w_1''w_1' + \frac{1}{2}(1-\nu)w_1'^2\cot\alpha\} \tag{3-53}$$

$$\begin{aligned}(1+\nu)[v_2'+v_2\cot\alpha-2w_2] + k[&-w_2^{IV}-2w_2'''\cot\alpha \\ &+ (1+\nu+\cot^2\alpha)w_2'' - (2-\nu+\cot^2\alpha)w_2'\cot\alpha] \\ &- \frac{\lambda_0}{4}[w_2''+w_2'\cot\alpha] = -\frac{1}{R}\{\frac{1}{2}(1+\nu)w_1'^2 \\ &+ w_1''[v_1'+\nu v_1\cot\alpha-(1+\nu)w_1] + w_1'[v_1'' \\ &+ (1+\nu)v_1'\cot\alpha-\nu v_1-(1+\nu)w_1'-(1+\nu)w_1\cot\alpha]\} \\ &+ \frac{\lambda_1}{4}[w_1''+w_1'\cot\alpha]\end{aligned} \tag{3-54}$$

Since the right hand sides of these equations are quadratic in the spherical harmonic of order n and its derivatives (except for the last two terms of Eq. (3-54)), it is reasonable to assume the unknowns to be of the type:

$$v_2 = \sum_{m=0}^{n} B_{2m} \frac{d}{d\alpha} [P_{2m}(\cos \alpha)] \qquad (3\text{-}55)$$

$$w_2 = \sum_{m=0}^{n} C_{2m} P_{2m}(\cos \alpha) \qquad (3\text{-}56)$$

where B_{2m} and C_{2m} are coefficients to be determined. The Eqs. (3-53) and (3-54) can be transformed into a more workable form by a few mathematical manipulations. The first step is to substitute the expressions for v_1, v_2, w_1, and w_2 into the equations; then a procedure similar to Timoshenko's[35] can be performed on the left hand sides of the equations. This leaves the left hand side of Eq. (3-53) as a derivative with respect to α. Use of the differential equation which spherical harmonics satisfy makes the right hand side of the equation a derivative as well, and the equation can be integrated. Application of the change of variables (3-50) and the differential recurrence formulae for the resulting Legendre polynomials gives the result:

$$\sum_{m=0}^{n} \{(\Gamma_{2m}+1+\nu) B_{2m} + (1+\nu) C_{2m}\} P_{2m}$$

$$= -\frac{1}{4R} [-(1+\nu) P_n'^2 + (1+\nu) P_{n-1}'^2 + 2n(1+\nu) P_n P_{n-1}' + n(1-\nu+2n) P_n^2] + D \qquad (3\text{-}57)$$

$$\sum_{m=0}^{n} \{-(1+\nu)(\Gamma_{2m}+2)B_{2m} + [-2(1+\nu) - k\Gamma_{2m}^2 + (3+\nu)\Gamma_{2m} + 2(1+\nu)] + \frac{\lambda_0}{4}(\Gamma_{2m}+2)]C_{2m}\}P_{2m}$$

$$= \frac{1}{2R}\{[(1+\nu) - 2K(1-\nu) + 2Kn(n+1)]P_n'^2$$

$$- [(1+\nu) + 2K(1-\nu) + 2Kn(n+1)]P_n'^2_1$$

$$- 2n[(1+\nu) + 2Kn(n+\nu)]P_nP'_{n-1}$$

$$- [n(3n+2)(1+\nu) + 2Kn^2(2n+1)(n+\nu)]P_n^2\}$$

$$- \frac{\lambda_1}{4}[(\Gamma_n+2)P_n] \qquad (3\text{-}58)$$

where D is a constant of integration, P_n and P_{2m} are Legendre polynomials, and primes denote differentiation with respect x. It is now evident that our choice of series for v_2 and w_2 is appropriate since the right hand sides of the equations (with the possible exception of the last quantity of Eq. (3-58)) consist of terms composed of even powers of x up to 2n. The lefthand sides of the equations are thus adequate since they also contain the same even powers of x. The numerical solution of this system of equations is then a matter of expressing the Legendre polynomials in powers of x and equating the coefficients of the individual powers of x on each side of the equations. It turns out that this reduces to successively solving two algebraic equations simultaneously for the undetermined constants B_{2m} and C_{2m}.

Now, let us look at the last quantity of Eq. (3-58). In case n is even, this quantity contains only even powers of x and all is well. However, should n be an odd number this quantity will be composed entirely of odd powers of x, which obviously are not encompassed by the lefthand

side of the equation. In this case λ_1 vanishes since the integrand of $V_3(u_1)$ is an odd function about the equator of the shell (about x = 0) which condition causes $V_3(u_1)$ to vanish upon integration. This eliminates these potentially troublesome odd powers of x from the equation.

Once the coefficients, B_{2m} and C_{2m}, are calculated, the series for v_2 and w_2 are completely determined and we are able to evaluate the integrals necessary for obtaining λ_2. The expression for $V_{21}(u_1,u_2)$ is obtained by applying expansions of the form of Eq. (2-5) to $V_3(u)$ and isolating the terms which are fourth order in ϵ. $V_4(u_1)$ is, of course, the expression (3-37) with w replaced by w_1, and $V_2^{\lambda}(u_1)$ is as before. λ_2 is then calculated from Eq. (2-33).

CHAPTER IV

DISCUSSION OF THEORETICAL RESULTS

Because of the complexity of the computations involved the high speed digital computer was used for the numerical portion of this investigation. Furthermore, the largeness of the coefficients of the Legendre polynomials of higher order and the fact that the coefficients alternate in sign necessitated the use of multiple-precision arithmetic on the computer for most of the calculations. "Triple-precision"—approximately 25 significant figure—subroutines were programmed and used for calculations on shells with radius/thickness ratios greater than 50. Available "double-precision" subroutines were used on shells having a radius/thickness ratios from 14 to 50.

The numerical values of the load perturbation coefficients obtained for a Poisson's ratio of 0.5 are given in Table I and are presented graphically in Figs. 1 to 3. In the figures the curves serve to associate the individual points and to indicate the trend the points are taking; the curves are not meant to represent a spectrum of points between those indicated since such is not the case. It can be seen that for n even, λ_1 is tending to zero in an asymptotic manner as the shell becomes thinner. If for a thin enough shell λ_1 does in fact vanish, the second perturbation coefficient λ_2 would have to be calculated in order to determine the stability or instability of the shell. With but one exception, and this for a very thick shell, λ_2 is negative and decreases

further for thinner and thinner shells. This indicates that complete, thin spherical shells subjected to uniform external pressure are inherently unstable at the Euler buckling load, as amply verified by all available experimental evidence.

The coefficients of the expansions for v_2 and w_2 are given in Tables II and III.

At no place have boundary conditions been mentioned since we have considered only complete spherical shells; nevertheless, by our exclusion of Legendre polynomials (or spherical harmonics) of the second kind in our solution we have tacitly demanded the regularity of our solution throughout the region.

This investigation furnishes information which can describe the behavior of a thin spherical shell under external pressure in an indirect manner only. The instability of the shell at the Euler load is established; however, further information is necessary in order to establish a more realistic buckling load for the shell. Application of a theory incorporating the effects of initial imperfections may shed new light on the subject as may the investigation of the third load perturbation coefficient, λ_3, as suggested in Chapter II. This latter investigation might produce a realistic buckling load as proposed by Friedrichs[12] and Tsien.[33]

In the light of the fact that all available experiments show a region of buckling over but a small portion of the sphere, one would expect the effect of displacement perturbation functions u_2, u_3, etc., to

tend to diminish the displacements described by the linear buckling mode u_1 over the portion of the sphere away from a main buckling dimple. In particular, it would be expected that the second perturbation function u_2 would tend to minimize the displacements in the neighborhood of the equator of the spherical shell. A few preliminary calculations (for very thick shells, n = 2 and n = 3) involving the radial displacement functions w_2 indicate that this indeed is the case for certain values of the perturbation parameter ϵ. The effect of the perturbation functions on the displacements of the linear buckling mode is, of course, dependent upon the parameter ϵ. The functions w_2 are even functions about the equator and their effect at the poles is to augment the linear displacements there in case the buckling mode is an even function about the equator, and to augment the linear displacements at one pole and diminish them at the other pole for a buckling mode which is an odd function about the equator.

In addition the buckling mode which produced the minimum buckling load for a vanishing perturbation parameter ϵ was used in each case. It is possible that the buckling mode for a minimum load changes as the parameter ϵ takes on larger and larger values. This possibility affords a topic for further investigation.

The conclusions reached here concerning the buckling behavior of thin spherical shells are in contrast to those which may be reached concerning the buckling behavior of plates. In the case of plates the first load perturbation coefficient λ_1 vanishes and the second coef-

ficient λ_2 is positive. This shows, of course, that plates have equilibrium configurations adjacent to the unbuckled state available only at loads greater than the Euler load and are thereby stable.

Koiter,[19] using a perturbation analysis similar to the one used here, has shown that very narrow circular panels supported at the edges and subjected to axial loading are stable and behave in a manner similar to plates. However, when the panel's curvature reaches a certain value, the panel becomes unstable at the Euler buckling load and thus behaves like a complete cylindrical shell.

CHAPTER V

EXPERIMENTAL APPARATUS AND PROCEDURE

Four different hemispherical shells were tested in the course of the investigation; one was a portion of a child's toy ball while the remaining three were fabricated specially for this testing program. The displacements of the various points on the external surface of the shells were measured using photographs.

For testing, each shell was mounted and sealed on a rigid base plate in which was a displacement plunger threaded and calibrated so that the displacement on the interior of the shell could be controlled easily and accurately. A "bleeder" valve (for the escape of air trapped in filling the shell with water) and a hose connection for a manometer lead were also mounted on the base plate. Points along a meridian were marked with India ink on the hemispherical shell at intervals of 2-1/2 or 5 degrees depending on the size of the shell and the distance from the apex, or pole, of the shell. The experimental setup is shown in Fig. 4.

Photographs were taken of the shell in the various stages of buckling, i.e., in the undeformed state, in several pre-buckling deformed states, and in several buckled states. In some cases, indicated by the point's being enclosed by triangles on the graphs, the displacement medium was reintroduced in order to observe the "unbuckling" deflections

and pressures. The shell was returned to the undeflected state after each picture was taken.

Used for the photographic work was a Graflex Speed Graphic camera employing 4 by 5 in. sheet film. In order to minimize possible distortion a small lens opening was used and the plane of the film was oriented parallel to the plane of the points marked on the shell. Avoidance of the effects of heat from photoflood lamps was accomplished by using an electric flash gun for illumination. The camera setup is shown in Fig. 5.

Water was the displacement medium used in the case of the toy ball shell which was made of one of the modern plastics with a Young's modulus of 640 lb/sq in. The radius of the shell was 3 in., the average thickness was 0.054 in., and the mean deviation from this thickness was 0.0047 in. The pressure difference between that on the outside and that on the inside of the shell was measured using a manometer tube open to the atmosphere. The manometer fluid was water which was common to the water inside the shell.

The three rubber shells used each had a radius of 4-1/2 in. and had nominal thickness of 0.030 in., 0.060 in., and 0.100 in. Their average thicknesses were 0.029 in., 0.062 in., and 0.099 in., and the mean deviations from these were 0.0007 in., 0.0018 in., and 0.0035 in., respectively. The shells were made by a rubber dipping process, i.e., the rubber was deposited on a hemispherical form immersed in a liquid latex solution; consequently, there was no concern about initial resid-

ual stresses in the shells. The Young's modulus of the rubber is 340 lb/sq in. Air was the displacement medium used in these tests and an inclined tube alcohol manometer was used for pressure measurement. It was found that using one's lungs to control the displacement volume was more convenient than using the threaded plunger for these tests.

A photographic enlarger was used to measure the deflections of the shells as recorded on film. The image of the deflected shell was cast upon the positive photographic picture of polar coordinate paper. The distances of the images of the points from lines of the coordinate paper were measured, recorded, and compared with the distances of corresponding points of the undeflected shell in order to obtain the displacements of the points of the shell. Both radial and tangential displacements of the points on the surface of the shells were measured in this manner. A typical picture of a buckled shell is shown in Fig. 6.

In order to obtain the tangential displacements of the neutral surface of the shell, the tangential displacements of the outer surface were modified according to the formula:

$$v_o = v_s + \frac{h}{2R}\frac{dw}{d\alpha} \qquad (5\text{-}1)$$

where:

v_o = tangential displacement of neutral surface

v_s = tangential displacement of outside surface

Thus, the Euler-Bernoulli hypothesis that "normals to the undeformed middle surface are deformed, without extension, into normals to the de-

formed middle surface" was invoked. No such modification was needed for the radial displacements.

Measurement of the moduli of elasticity of the plastic of the toy ball and of the rubber of the remaining three shells was accomplished on an Instron testing machine so that the elongation of the specimens never exceeded three percent. The maximum stress encountered in the case of the plastic was 13.3 psi and of the rubber 8.8 psi. These compare to theoretical buckling stresses of 7.8 psi and 5.0 psi for the toy ball and the thickest rubber shell respectively.

CHAPTER VI

EXPERIMENTAL RESULTS AND DISCUSSION

The plots of displacement, both radial and tangential, versus polar angle, Figs. 11-18, show rather conclusively two significant properties of the shape of the dimple formed in the buckling of a thin spherical shell, namely that the displacements are axially symmetric and that there is a region just outside the region of the dimple produced upon buckling where small but very definite negative (outward) radial displacements exist. It was observed visually that the axisymmetry of the displacements degenerated considerably when the shell was displaced far beyond the state of first buckling; however, from the character of the displacements it seemed quite obvious that the lack of symmetry was due to imperfections in the shell rather than the inherent nature of the buckling phenomenon. Thus, the assumption of axisymmetry made in the course of the theoretical analysis is now fortified on the basis of the experimental evidence gathered.

L. H. Donnell[11] first observed the above mentioned negative radial displacements which are very evident in the plots. That there are negative tangential displacements associated with these is not shown quite so convincingly in the figures due to the fact that the tangential displacements were considerably smaller than the radial displacements thus making their measurement relatively less accurate. In addition the photographic images of the points on the shells appeared longer in the tan-

gential direction than in radial direction so that measurements in the tangential direction were a bit less accurate. (Note that for the sake of continuity at the origin the tangential displacements have been plotted positive downward to the left of the origin.)

Some preliminary work (for the toy ball displacement data) was done to try to describe the shape of the buckled shell mathematically. A great degree of success was achieved for the radial displacements as can be seen in the overlay Fig. 11a. The curves in this figure are plotted from the expression:

$$w = w_o \exp\left[-(21.4w_o+10.1)\alpha^{(3.42w_o+1.54)}\right] \cos \frac{3.48}{w_o+0.483}\alpha \qquad (6\text{-}1)$$

where w_o is the maximum radial displacement and "exp" denotes that e, the base of the natural logarithms, is to be raised to the power represented by the expression in the brackets which follow it. An expression for the tangential displacements patterned after expression (6-1) does not describe the experimental values nearly as well as (6-1) describes the radial displacements. This expression, which is plotted in Fig. 12a, is:

$$v = \frac{w_o-0.07}{5.8} \exp\left[-(21.4w_o+10.1)\alpha^{(3.42w_o+1.54)}\right] \sin \frac{3.48}{w_o+0.483}\alpha \qquad (6\text{-}2)$$

These expressions, (6-1) and (6-2) were developed so that they might serve as a guide in the establishment of an approximate large deflection shell theory as outlined in Ref. 10.

The experimental load-displacement curves, Figs. 7-10 (the number adjacent to each point indicates the picture in Figs. 11-18 which corresponds to the point), conform quite well with the shape generally drawn to represent the shell-buckling phenomenon.[34,etc.] The deflection prior to buckling increases more or less linearly, and upon buckling the load drops to a markedly smaller value while the displacements remain largely unchanged. One definite difference is observed, however, in that the load does not increase for extremely large displacements. In one case (Test No. 5) the maximum deflection exceeded half the radius of the shell with no hint of the load's ever increasing. This indicates that an evaluation of the third load perturbation coefficient λ_3 may not be fruitful as was previously suggested. Such an analysis would give a definite relative minimum on a plot of the load versus the perturbation parameter ϵ.

The buckling loads observed during the course of this investigation compare not unfavorably with the buckling loads predicted by the linear theory. In Table IV are tabulated the linear buckling load, the observed buckling load, and the percent the experimental load is of the theoretical. The expression for the buckling load according to the linear theory, of course, is:

$$p_{cr} = \frac{2Eh^2}{R^2\sqrt{3(1-\nu^2)}} \qquad (6\text{-}3)$$

It can be seen that the experimental buckling load is greater than half in each case and in one case greater than three-quarters of the theo-

retical buckling load. Although the data obtained from only four specimens are admittedly quite meager, one would be led to attribute the discrepancies between the experimental and the theoretical results to imperfections in the shells rather than to an improper theoretical approach.

It should be noted that although a complete spherical shell was not used, very little error in the displacements or the buckling loads should have been introduced since the dimpling occurred in only a small sector of the hemispherical specimens used.

For each of the four of the shells tested a slight dimpling was observed prior to the explosive snap-through buckling action of the shell. It is suspected that this phenomenon is attributable to initial imperfections in the shell. The pictures were taken at the point on the shell where it had been established previously that the buckling would take place. Consequently, if imperfections do dictate the location of the buckle, any effect of the imperfections at the point would certainly be observed before the actual buckling. In any case there was a definite and uncontrollable snap-through buckling of the shell. This occurred even when water was used as the displacement medium and the manometer was isolated from the system. This explosive type of buckling tends to confirm the findings of the theoretical investigation which indicate instability at the Euler load.

CHAPTER VII

CONCLUSIONS

1. The mathematical perturbation analysis of the buckling problem for a complete, uniformly thick, thin spherical shell shows that the shell is unstable at the classical, or Euler buckling load regardless of whether the linear buckling mode is an even or an odd function about the equator of the shell.

2. The laboratory use of photographic methods for displacement measurements has shown the existence of a region of small but very definitely outward radial displacements just outside the main buckling dimple.

3. Furthermore, the buckling displacements observed in the course of the experimental program conducted using hemispherical specimens are symmetric in nature.

4. Although no conclusions concerning the buckling loads of actual shells can be drawn from tests on only four specimens, the buckling loads experienced tend to indicate that the classical linear buckling load is the correct one.

REFERENCES

1. Archer, R. R., "Stability Limits for a Clamped Spherical Shell Segment Under Uniform Pressure," Quart. Appl. Math., vol. 15, no. 4, January, 1958, pp. 355-366.

2. Ashwell, D. G., "On the Large Deflexion of a Spherical Shell with an Inward Point Load," Proceedings of the I.U.T.A.M. Symposium on The Theory of Thin Elastic Shells, North-Holland Publishing Company, Amsterdam, 1960, pp. 43-63.

3. Biezeno, C. B., "Über die Bestimmung der Durchschlagkraft einer schwachgerkrümmten kreisförmigen Platte," Z. angew. Math. Mech., vol. 15, 1935, p. 10.

4. Biezeno, C. B., and Grammel, R., Engineering Dynamics, vol. 2, Blackie, London, 1956, p. 484.

5. Budiansky, B., "Buckling of Clamped Shallow Spherical Shells," Proceedings of the I.U.T.A.M. Symposium on The Theory of Thin Elastic Shells, North-Holland Publishing Company, Amsterdam, 1960, pp. 64-94.

6. Budiansky, B., and Weinitschke, H. J., "On Axisymmetrical Buckling of Clamped, Shallow, Spherical Shells," J. Aero. Sci., vol. 27, no. 7, July, 1960, pp. 545-546.

7. Chien, W. Z., "The Intrinsic Theory of Thin Shells and Plates," Quart. Appl. Math., vol. 2, no. 2, July, 1944, pp. 120-135.

8. Chien, W. Z., and Hu, H. C., "On the Snapping of a Thin Spherical Cap," 9th International Congress of Applied Mechanics, University of Brussels, vol. 6, 1957, pp. 309-320.

9. Courant, R., and Hilbert, D., Methods of Mathematical Physics, Interscience Publishers, Inc., New York, 1953.

10. Donnell, L. H., "Shell Theory," Proceedings of the Fourth Midwestern Conference on Solid Mechanics, The University of Texas, Austin, September, 1959, pp. 1-13.

11. Donnell, L. H., "Large Displacement Shell Theory," Illinois Institute of Technology Department of Mechanics Report No. 2-2, Chicago, August, 1960.

REFERENCES (Continued)

12. Friedrichs, K. O., "On the Minimum Buckling Load for Spherical Shells," Theodore von Kármán Anniversary Volume, Cal. Inst. Tech., Pasadena, 1941, pp. 258-272.

13. Grigolyuk, E. I., "On the Unsymmetrical Snapping of Shells of Revolution," Proceedings of the I.U.T.A.M. Symposium on The Theory of Thin Elastic Shells, North-Holland Publishing Company, Amsterdam, 1960, pp. 112-121.

14. Hobson, E. W., The Theory of Spherical and Ellipsoidal Harmonics, Chelsea Publishing Company, New York, 1955.

15. Jahnke, E., and Emde, F., Tables of Functions, Dover Publications, New York, 1945, pp. 109-125.

16. Kaplan, A., and Fung, Y. C., "A Nonlinear Theory of Bending and Buckling of Thin Elastic Shallow Spherical Shells," NACA TN 3212, 1954.

17. Keller, H. B., and Reiss, E. L., "Spherical Cap Snapping," J. Aero. Sci. vol. 26, no. 10, October, 1959, pp. 643-652.

18. Klöppel, K., and Jungbluth, O., "Beitrag zum Durchschlagproblem dünnwandiger Kugelschalen," Der Stahlbau, vol. 25, no. 6, June, 1953, pp. 121-130.

19. Koiter, W. T., "Buckling and Post-Buckling Behaviour of a Cylindrical Panel under Axial Compression," Trans. Nat. Aero. Res. Inst., Amsterdam, vol. 20, 1955, pp. 71-84 (Report S.476).

20. Koiter, W. T., "Elastic Stability and Post-Buckling Behavior," presented at First All-Union Congress of Theoretical and Applied Mechanics, Moscow, 1960.

21. Murray, F. J., and Wright, F. W., "Buckling of Thin Spherical Shells," J. Aero. Sci., vol. 28, no. 3, March 1961, pp. 223-226.

22. Nash, W. A., and Modeer, J. R., "Certain Approximate Analyses of the Nonlinear Behavior of Plates and Shallow Shells," Proceedings of the I.U.T.A.M. Symposium on The Theory of Thin Elastic Shells, North-Holland Publishing Company, Amsterdam, 1960, pp. 331-354.

23. Reiss, E. L., "Axially Symmetric Buckling of Shallow Spherical Shells Under External Pressure," J. Appl. Mech., vol. 25, December, 1958, pp. 556-560.

REFERENCES (Continued)

24. Reiss, E. L., Greenberg, H. J., and Keller, H. B., "Nonlinear Deflections of Shallow Spherical Shells," J. Aero. Sci., vol. 24, no. 7, July, 1957, pp. 533-543.

25. Reissner, E., "Stresses and Small Displacements of Shallow Spherical Shells I," J. Math. Phys., vol. 25, no. 1, 1946, pp. 80-85.

26. Reissner, E., "Stresses and Small Displacements of Shallow Spherical Shells II," J. Math. Phys., vol. 25, 1947, pp. 279-300.

27. Reissner, E., "On the Theory of Thin Elastic Shells," Reissner Anniversary Volume, Contributions to Applied Mechanics, J. W. Edwards, Ann Arbor, Michigan, 1949, pp. 231-247.

28. Reissner, E., "On Axisymmetric Deformations of Thin Shells of Revolution," Proceedings of Symposia in Applied Mathematics, vol. 3, McGraw-Hill Book Company, Inc., New York, 1950, pp. 27-52.

29. Schwerin, E., "Zur Stabilität der dünnwandigen Hohlkugel unter gleichmässigem Aussendruck," Z. angew Math. Mech., vol. 2, 1922, p. 81.

30. Simons, R. M., "A Power Series Solution of the Nonlinear Equations for Axi-symmetrical Bending of Shallow Spherical Shells," J. Math. Phys., vol. 35, no. 2, July, 1956, pp. 164-176.

31. Thompson, J.M.T., "The Elastic Instability of a Complete Spherical Shell," The Aeronautical Quarterly, vol. 13, May, 1962, pp. 189-201.

32. Thurston, G. A., "A Numerical Solution of the Nonlinear Equations for Axisymmetric Bending of Shallow Spherical Shells," 10th International Congress of Applied Mechanics, Stresa, Italy, 1960.

33. Tsien, H. S., "A Theory for the Buckling of Thin Shells," J. Aero. Sci., vol. 9, no. 10, August, 1942, pp. 373-384.

34. Tsien, H. S., "Lower Buckling Load in the Non-linear Buckling Theory for Thin Shells," Quart. Appl. Math., vol. 5, no. 2, 1947, pp. 236-237.

35. Timoshenko, S., Theory of Elastic Stability, McGraw-Hill Book Company, Inc., New York, 1936.

REFERENCES (Concluded)

36. van der Neut, A., "De elastische stabiliteit van de dunwandige bol," Diss., Delft, 1932.

37. von Kármán, T., Dunn, L. G., and Tsien, H. S., "The Influence of Curvature on the Buckling Characteristics of Structures," J. Aero. Sci., vol. 7, no. 7, May, 1940, pp. 276-289.

38. von Kármán, T., and Tsien, H. S., "The Buckling of Spherical Shells by External Pressure," J. Aero. Sci., vol. 7, no. 2, December, 1939, pp. 43-50.

39. von Willich, G.P.R., "The Elastic Stability of Thin Spherical Shells," Proc. Am. Soc. Civil Eng., vol. 85, no. EM 1, January, 1959, pp. 51-65.

40. Wedellsborg, B. W., "Critical Buckling Load on Large Spherical Shells," Proc. Am. Soc. Civil Eng., vol. 88, no. ST 1, pp. 111-121.

41. Weinitschke, H. J., "On the Nonlinear Theory of Shallow Spherical Shells," J. Soc. Indust. Appl. Math., vol. 6, no. 3, September, 1958, pp. 209-232.

42. Weinitschke, H. J., "On The Stability Problem for Shallow Spherical Shells," J. Math. Phys., vol. 38, no. 4, January, 1960, pp. 209-231.

43. Zoelly, R., "Uber ein Knickproblem an der Kugelschale," Diss., Zürich, 1915.

TABLE I

THE LOAD PERTURBATION COEFFICIENTS

n	R/h	λ_o	$R\lambda_1$	$R^2\lambda_2$
2	3.05	0.561	-0.935	0.139
3	4.67	0.393	0	- 39.1
4	7.26	0.262	-0.542	- 11.6
5	10.6	0.183	0	- 75.3
6	14.5	0.134	-0.378	- 26.3
7	19.2	0.102	0	-137
8	24.5	0.0804	-0.290	- 47.9
9	30.5	0.0648	0	-219
10	37.2	0.0533	-0.236	- 76.4
11	44.5	0.0446	0	-321
12	52.5	0.0378	-0.198	-111
13	61.2	0.0325	0	-444
14	70.5	0.0282	-0.171	-154
15	80.5	0.0247	0	-587
16	91.2	0.0219	-0.150	-202
17	103	0.0194	0	-755

TABLE II

THE SERIES EXPANSION COEFFICIENTS FOR v_2

2m \ n	2	3	4	5	6	7	8	9	10	11	12	13	14	15	16	17
2*	0	-4.76	-1.93	-1.38	-1.20	-1.13	-1.12	-1.13	-1.16	-1.21	-1.26	-1.31	-1.37	-1.43	-1.49	-1.56
4	-0.112	-0.933	0	-3.06	-1.19	-0.772	-0.608	-0.527	-0.482	-0.457	-0.443	-0.437	-0.436	-0.438	-0.443	-0.449
6		-0.0672	-0.195	-1.38	0	-3.37	-1.19	-0.717	-0.530	-0.435	-0.379	-0.345	-0.322	-0.307	-0.296	-0.290
8			-0.0548	-0.0904	-0.314	-1.93	0	-3.86	-1.28	-0.734	-0.520	-0.411	-0.347	-0.306	-0.279	-0.259
10				-0.0478	-0.0570	-0.138	-0.447	-2.51	0	-4.42	-1.40	-0.774	-0.532	-0.409	-0.338	-0.292
12					-0.0430	-0.0419	-0.0799	-0.193	-0.588	-3.10	0	-5.00	-1.54	-0.825	-0.553	0.417
14						-0.0395	-0.0336	-0.0542	-0.108	-0.252	-0.732	-3.70	0	-5.59	-1.67	-0.881
16							-0.0367	-0.0284	-0.0404	-0.0708	-0.140	-0.313	-0.878	-4.31	0	-6.19
18								-0.0344	-0.0249	-0.0321	-0.0508	-0.0896	-0.173	-0.377	-1.03	-4.91
20									-0.0325	-0.0224	-0.0268	-0.0390	-0.0630	-0.110	-0.207	-0.441
22										-0.0309	-0.0204	-0.0230	-0.0314	-0.0474	-0.0763	-0.131
24											-0.0295	-0.0189	-0.0203	-0.0262	-0.0373	-0.0566
26												-0.0283	-0.0176	-0.0182	-0.0225	-0.0305
28													-0.0272	-0.0166	-0.0166	-0.0197
30														-0.0263	-0.0157	-0.0153
32															-0.0254	-0.0150
34																-0.0246

*The coefficients B_0 are undetermined.

TABLE III

THE SERIES EXPANSION COEFFICIENTS FOR w_2

2m \ n	2	3	4	5	6	7	8	9	10	11	12	13	14	15	16	17
0	0.300	0.429	0.556	0.682	0.807	0.933	1.06	1.18	1.31	1.43	1.56	1.69	1.81	1.94	2.06	2.19
2	0	17.7	7.44	5.56	5.00	4.88	4.94	5.10	5.32	5.58	5.87	6.18	6.50	6.82	7.17	7.51
4	0.680	12.0	0	40.1	15.9	10.6	8.64	7.70	7.25	7.04	6.97	7.01	7.10	7.24	7.41	7.61
6		0.451	5.01	38.1	0	93.6	33.5	20.5	15.5	13.0	11.6	10.8	10.2	9.94	9.77	9.70
8			0.456	3.59	14.7	92.0	0	185	61.8	35.8	25.7	20.7	17.7	15.9	14.7	13.9
10				0.483	3.05	9.54	32.5	183	0	323	103	57.4	39.8	31.0	25.9	22.7
12					0.515	2.80	7.46	19.6	60.8	322	0	518	160	86.4	58.4	44.5
14						0.547	2.67	6.40	14.5	34.9	102	517	0	781	235	124
16							0.579	2.60	5.78	11.9	24.7	56.5	159	780	0	1120
18								0.610	2.57	5.39	10.3	19.6	38.9	85.6	234	1120
20									0.640	2.56	5.13	9.31	16.5	30.0	57.5	123
22										0.669	2.57	4.96	8.62	14.6	24.8	43.5
24											0.697	2.58	4.84	8.13	13.2	21.4
26												0.724	2.60	4.75	7.77	12.2
28													0.750	2.63	4.70	7.50
30														0.775	2.66	4.66
32															0.800	2.69
34																0.824

TABLE IV

COMPARISON OF THEORETICAL AND EXPERIMENTAL CRITICAL LOADS

Specimen	Critical Load (in. H_2O)		$\frac{\text{Exp. Crit. Load}}{\text{Theor. Crit. Load}} \times 100$ (%)
	Theoretical	Experimental	
Toy ball	7.92	5.13	65
Midwest - 0.030"	0.520	0.318	61
Midwest - 0.060"	2.37	1.21	51
Midwest - 0.100"	6.05	4.88	81

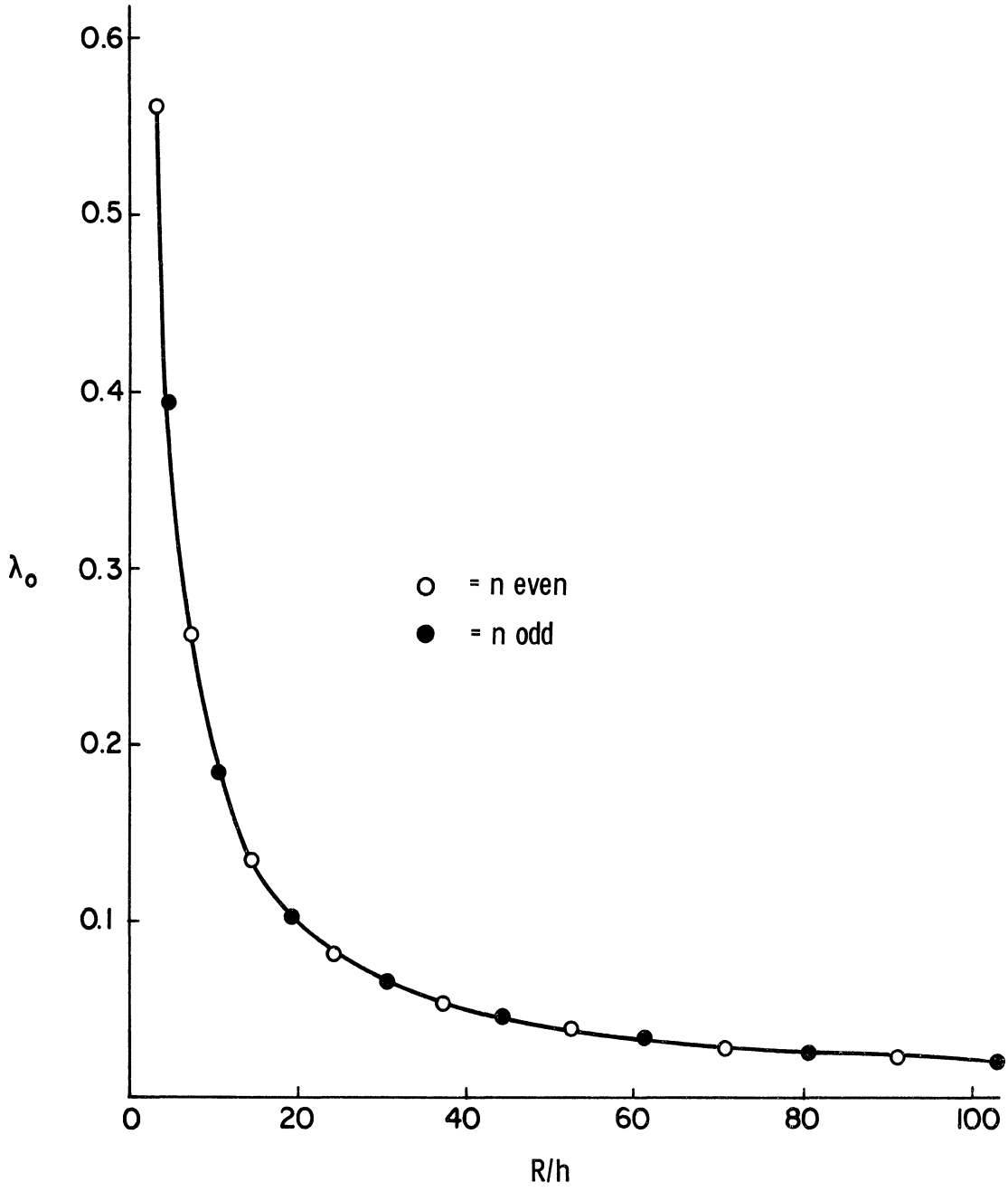

Fig. 1. The variation of the linear buckling load parameter with the radius/thickness ratio.

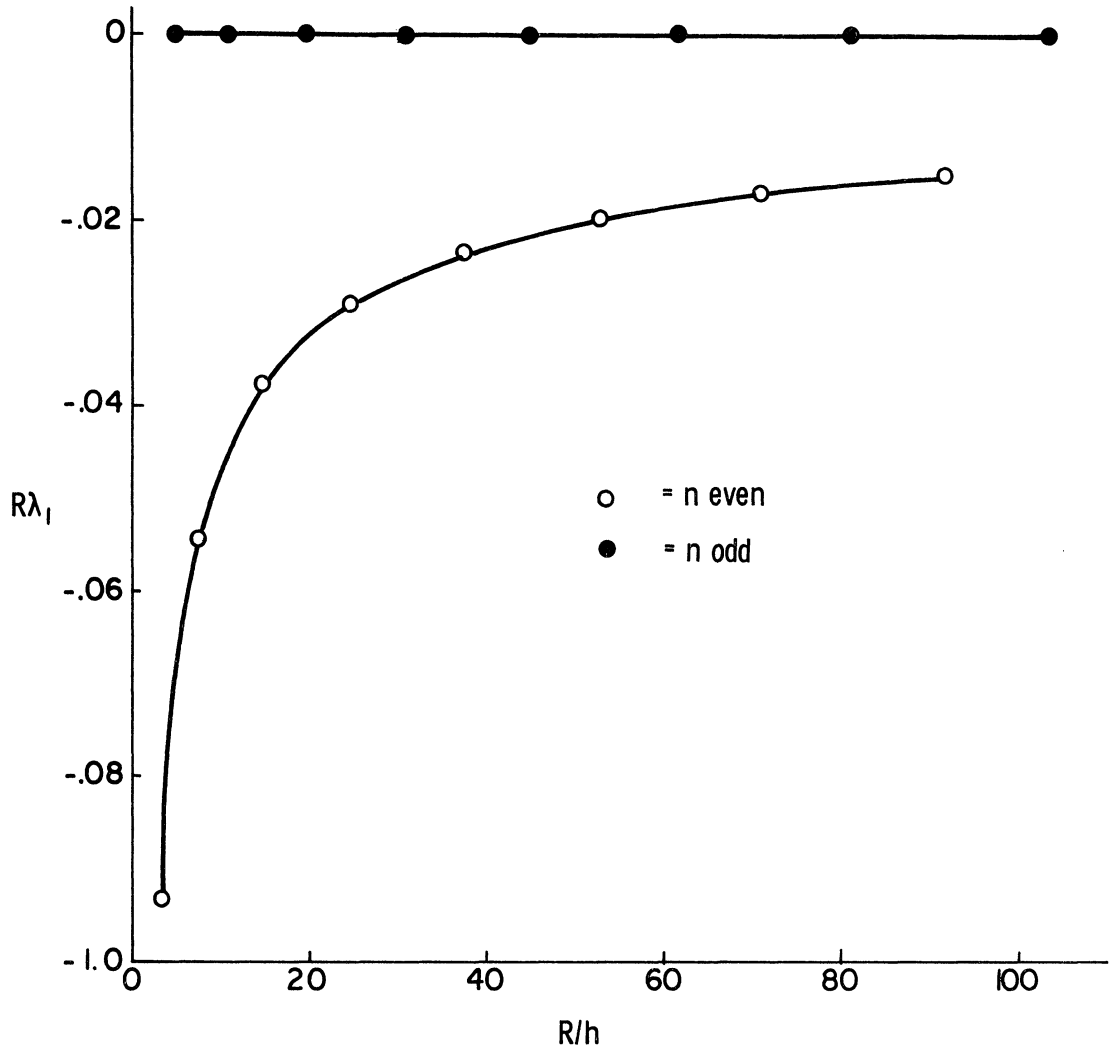

Fig. 2. The variation of the first load perturbation coefficient with the radius/thickness ratio.

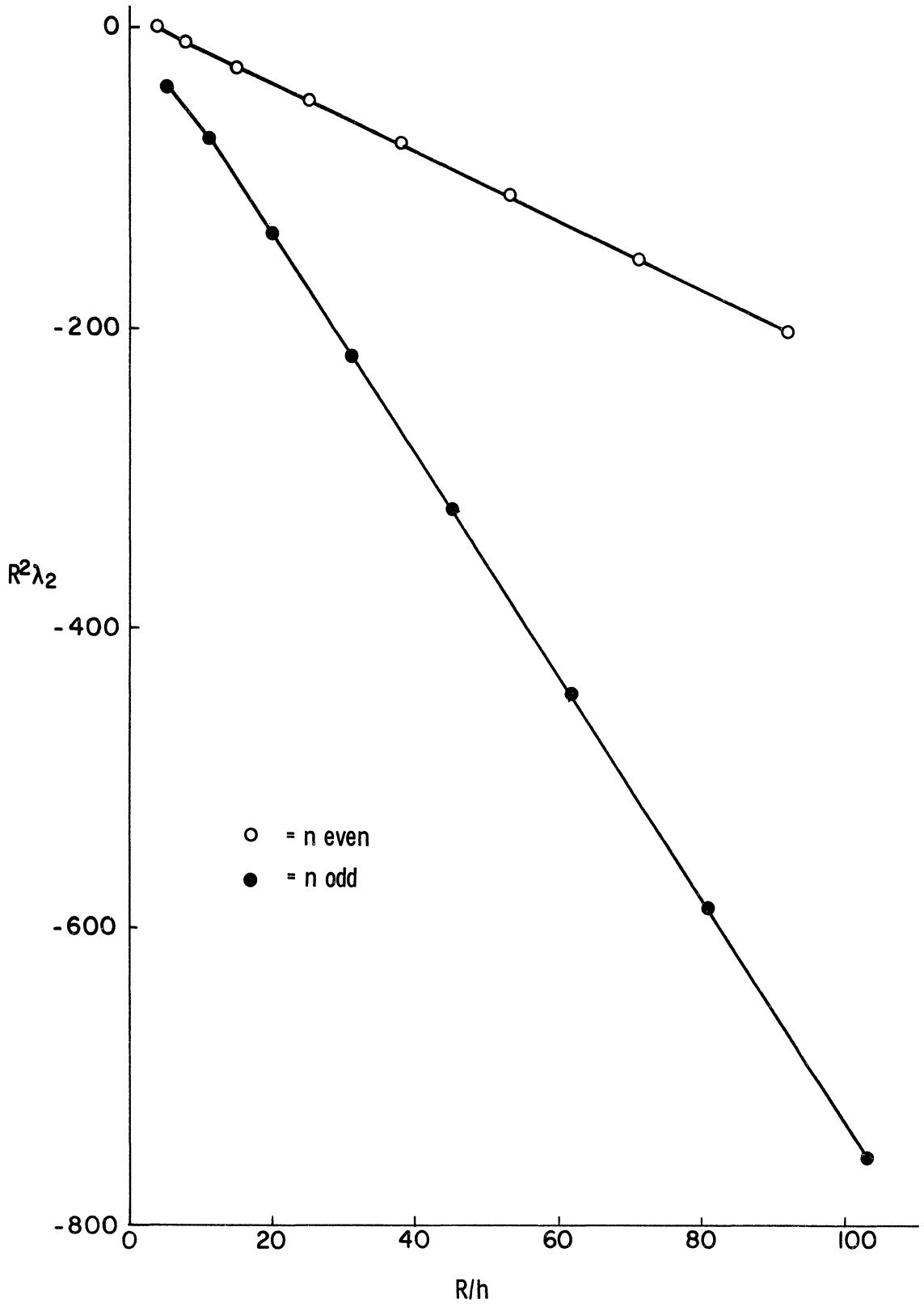

Fig. 3. The variation of the second load perturbation coefficient with the radius/thickness ratio.

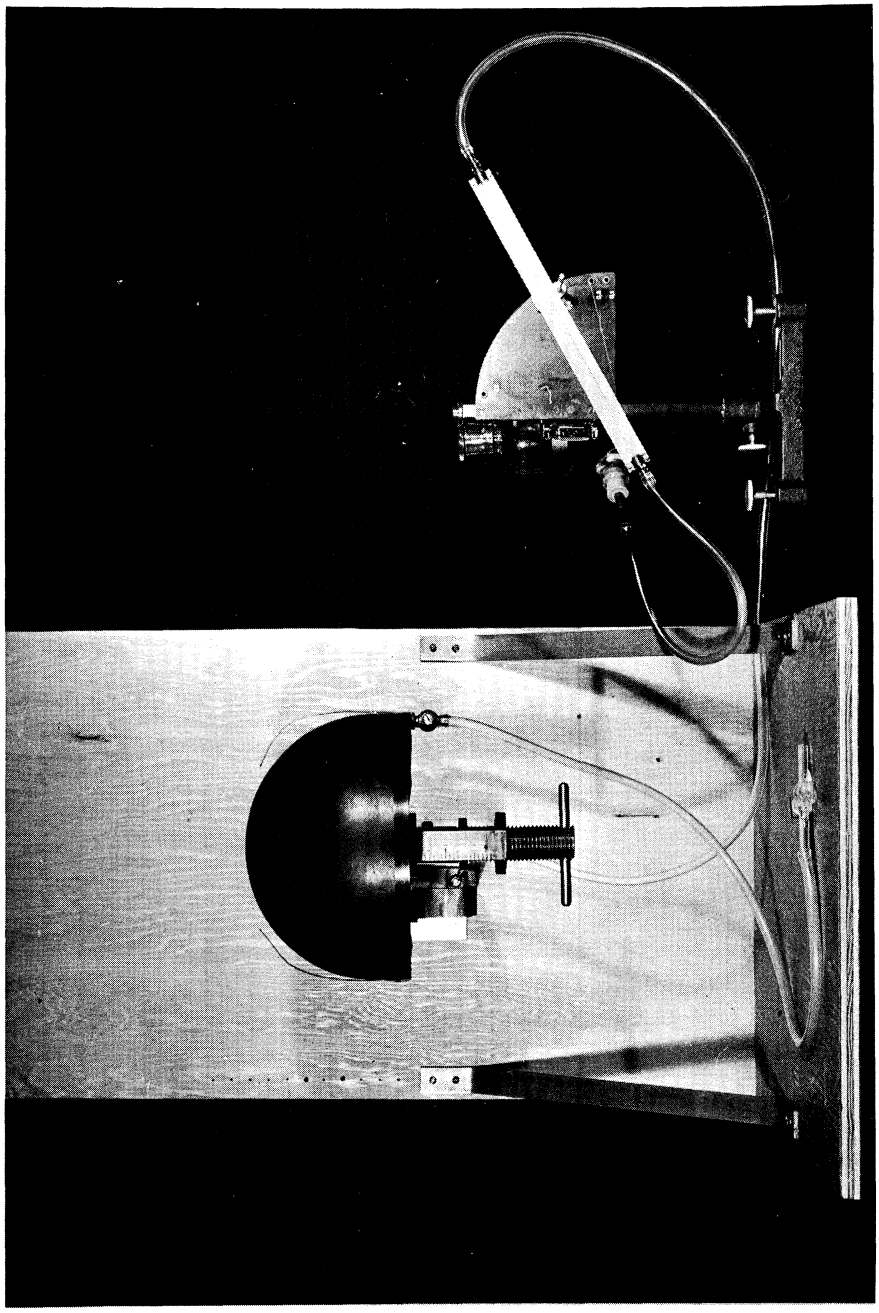

Fig. 4. Experimental apparatus.

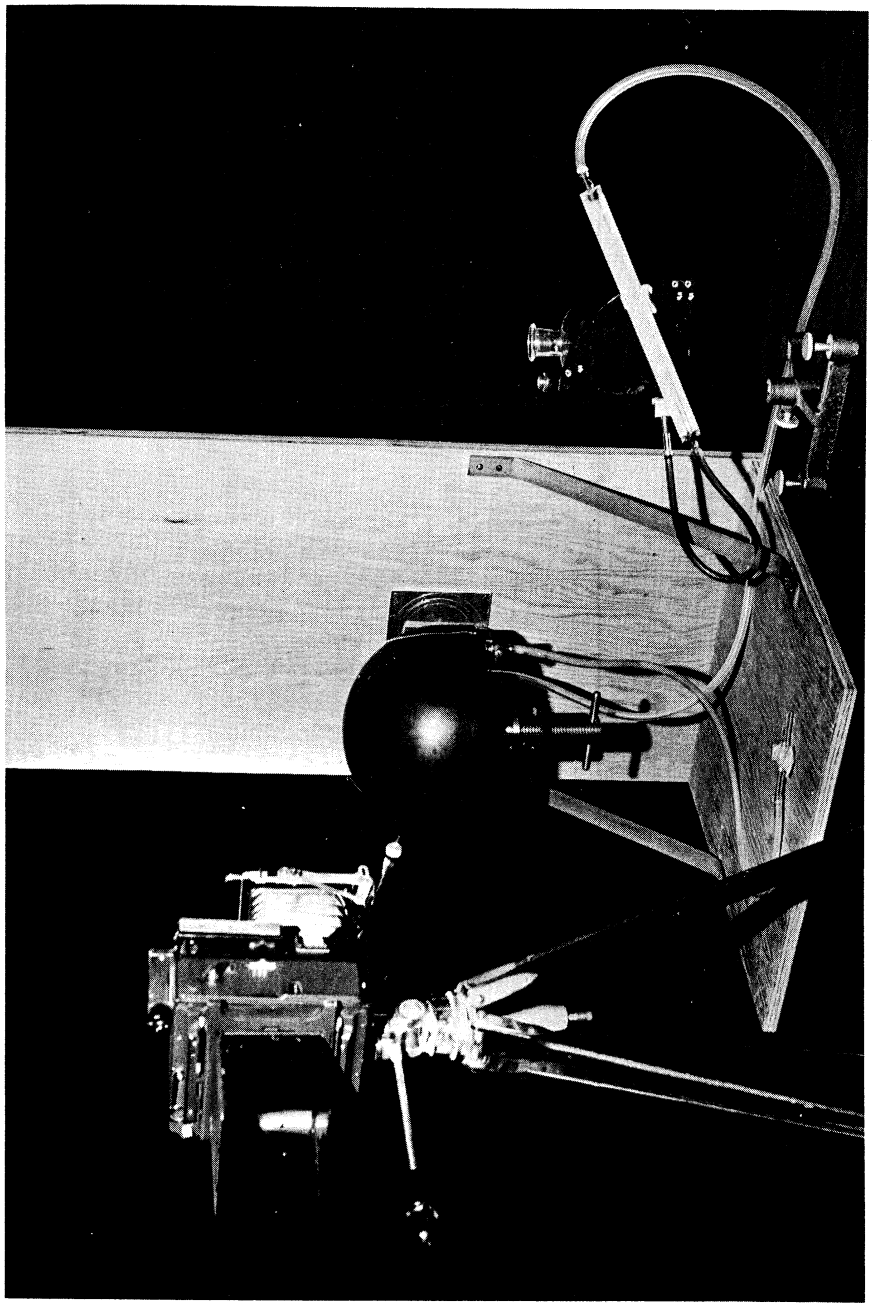

Fig. 5. Experimental apparatus with camera in place.

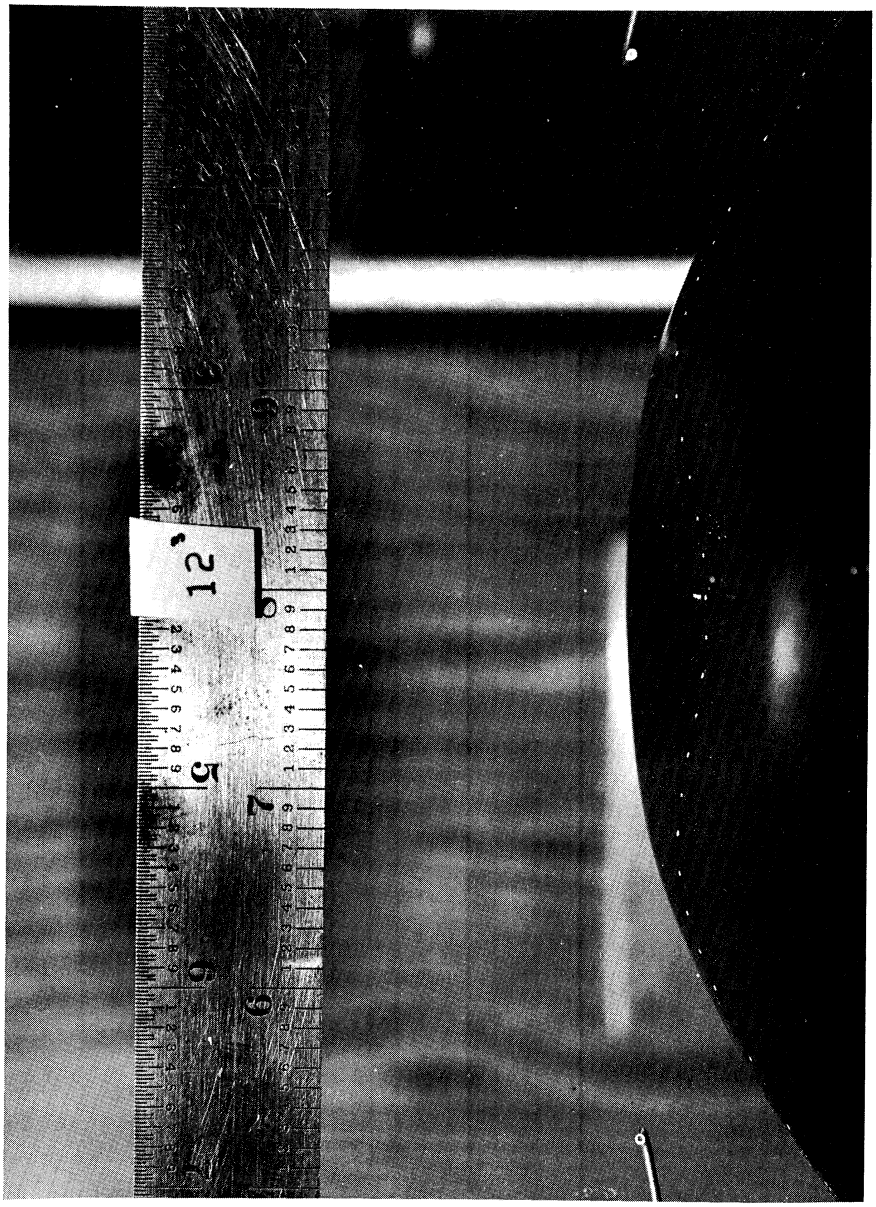

Fig. 6. Typical spherical shell displacement photograph.

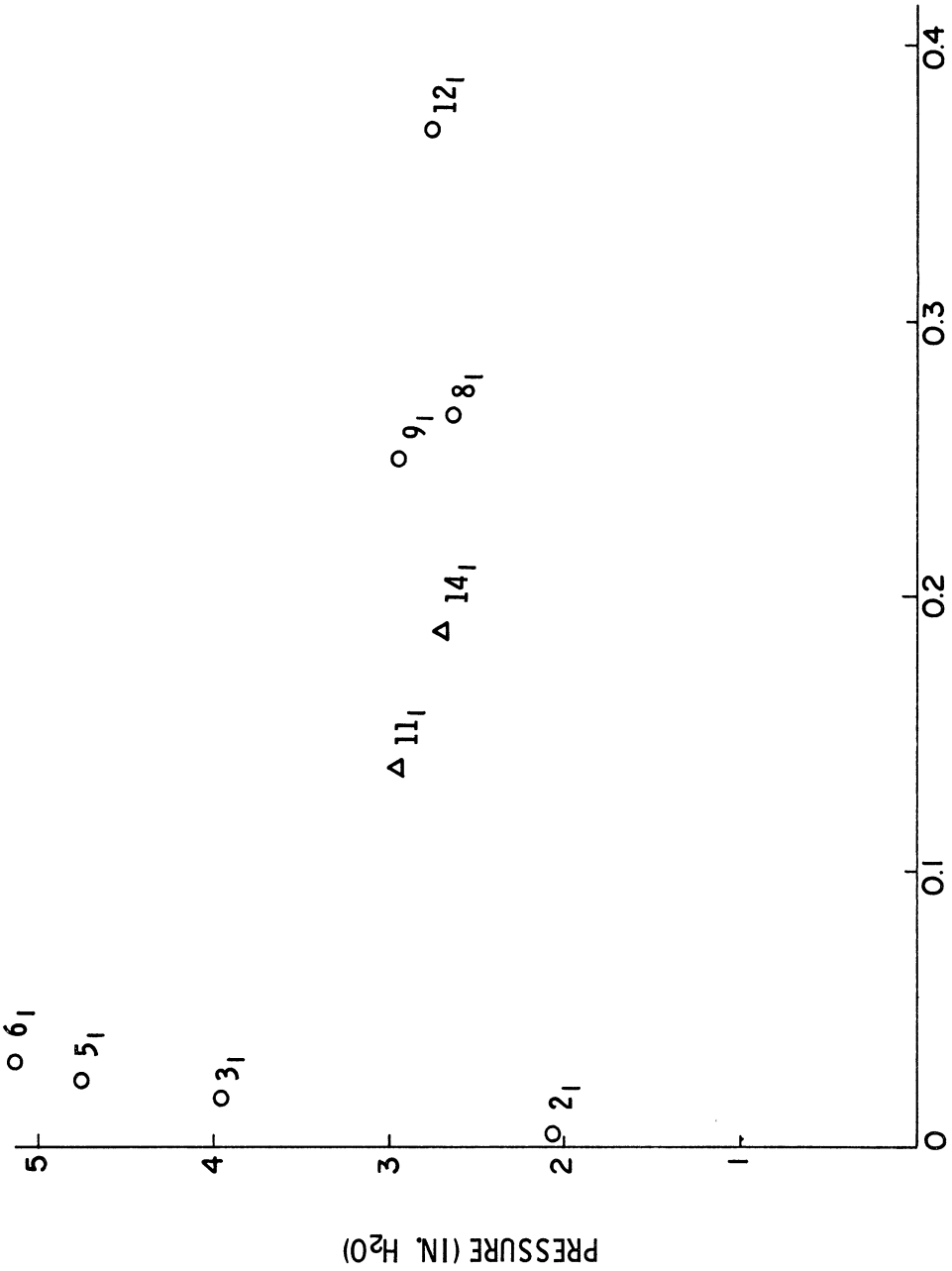

Fig. 7. Pressure vs. maximum radial displacement—toy ball shell, Test No. 1.

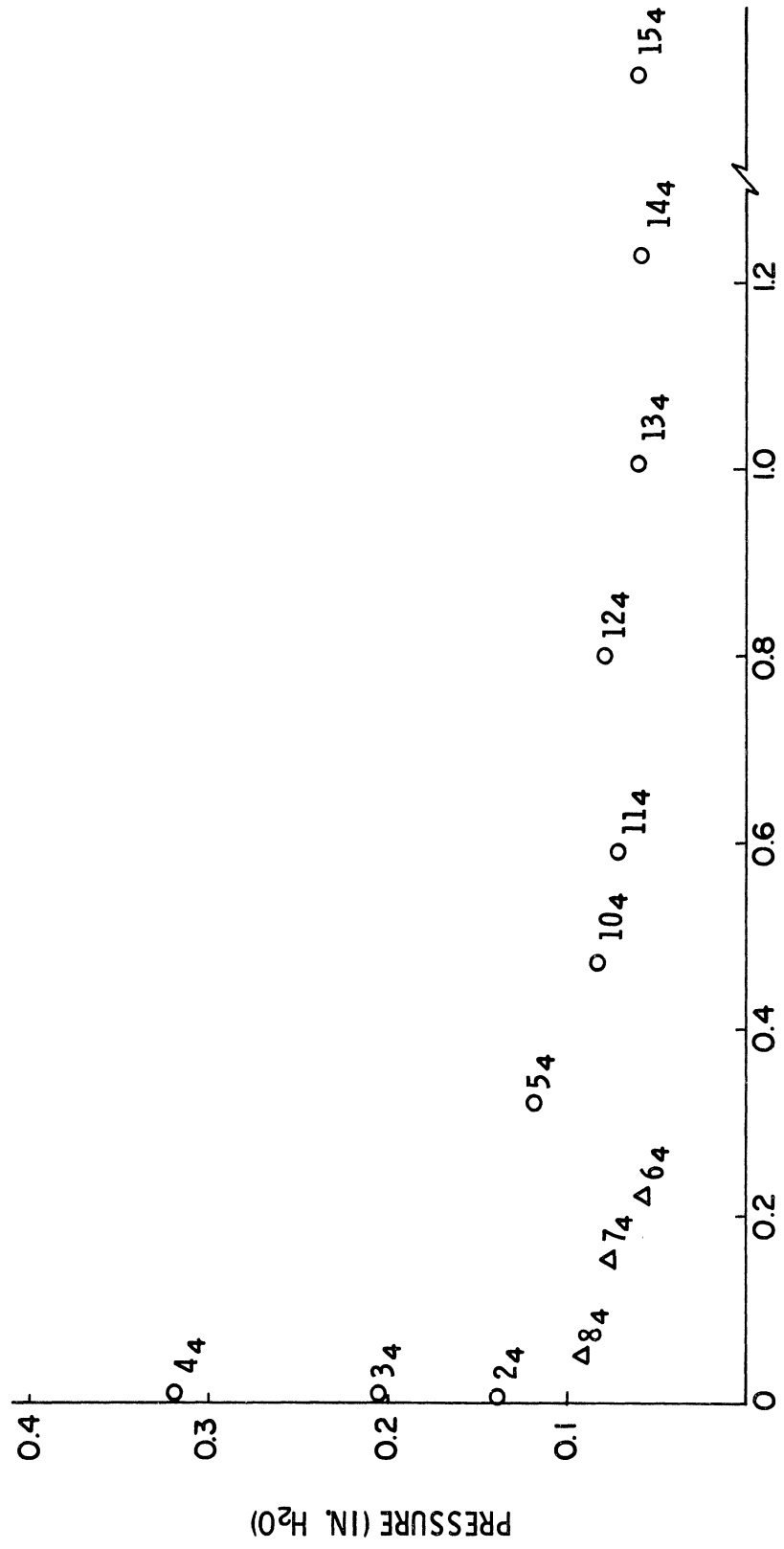

Fig. 8. Pressure vs. maximum radial displacement—Midwest shell No. 1 (0.030 in.), Test No. 4.

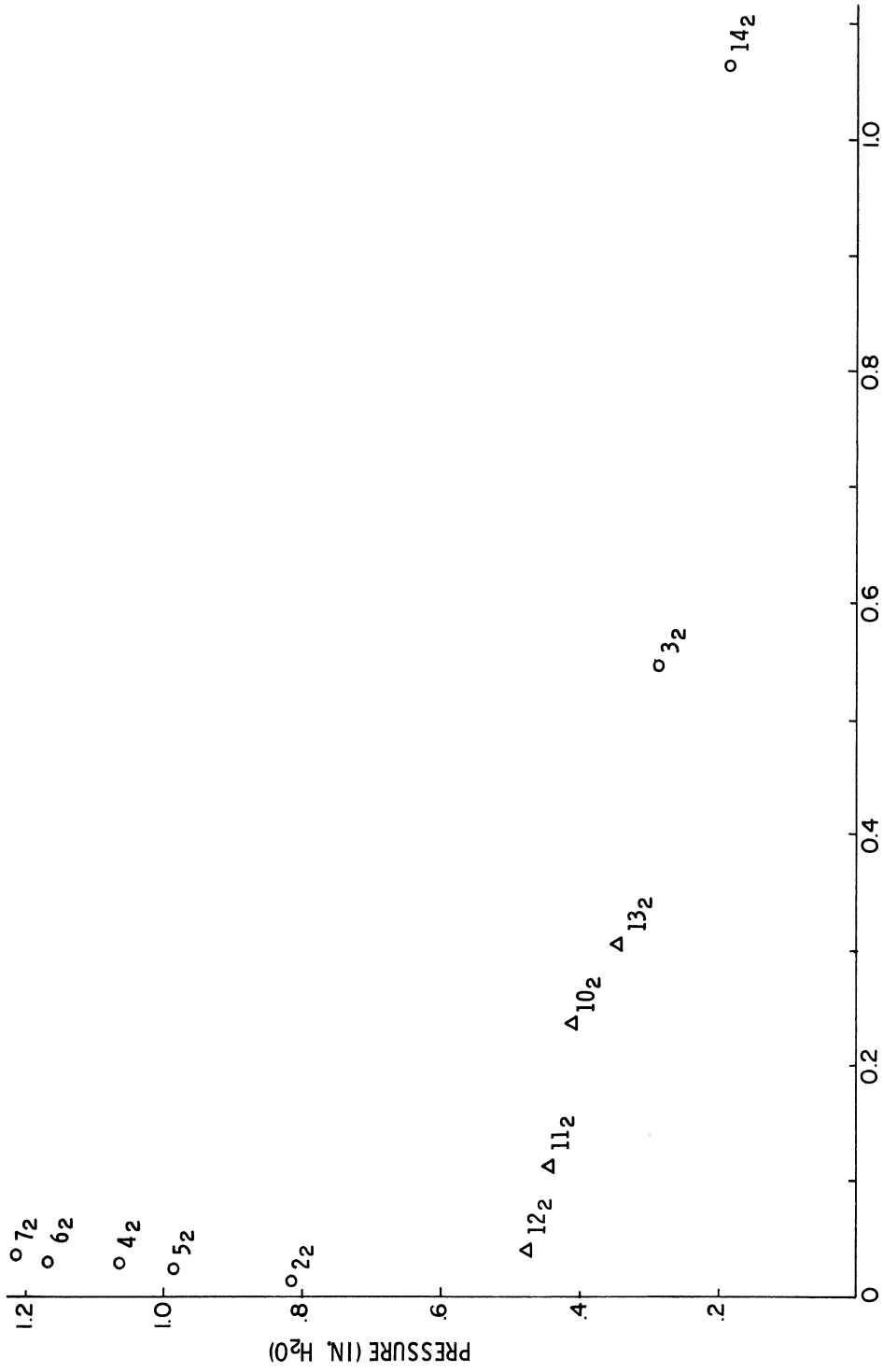

Fig. 9. Pressure vs. maximum radial displacement—Midwest shell No. 2 (0.060 in.), Test No. 2.

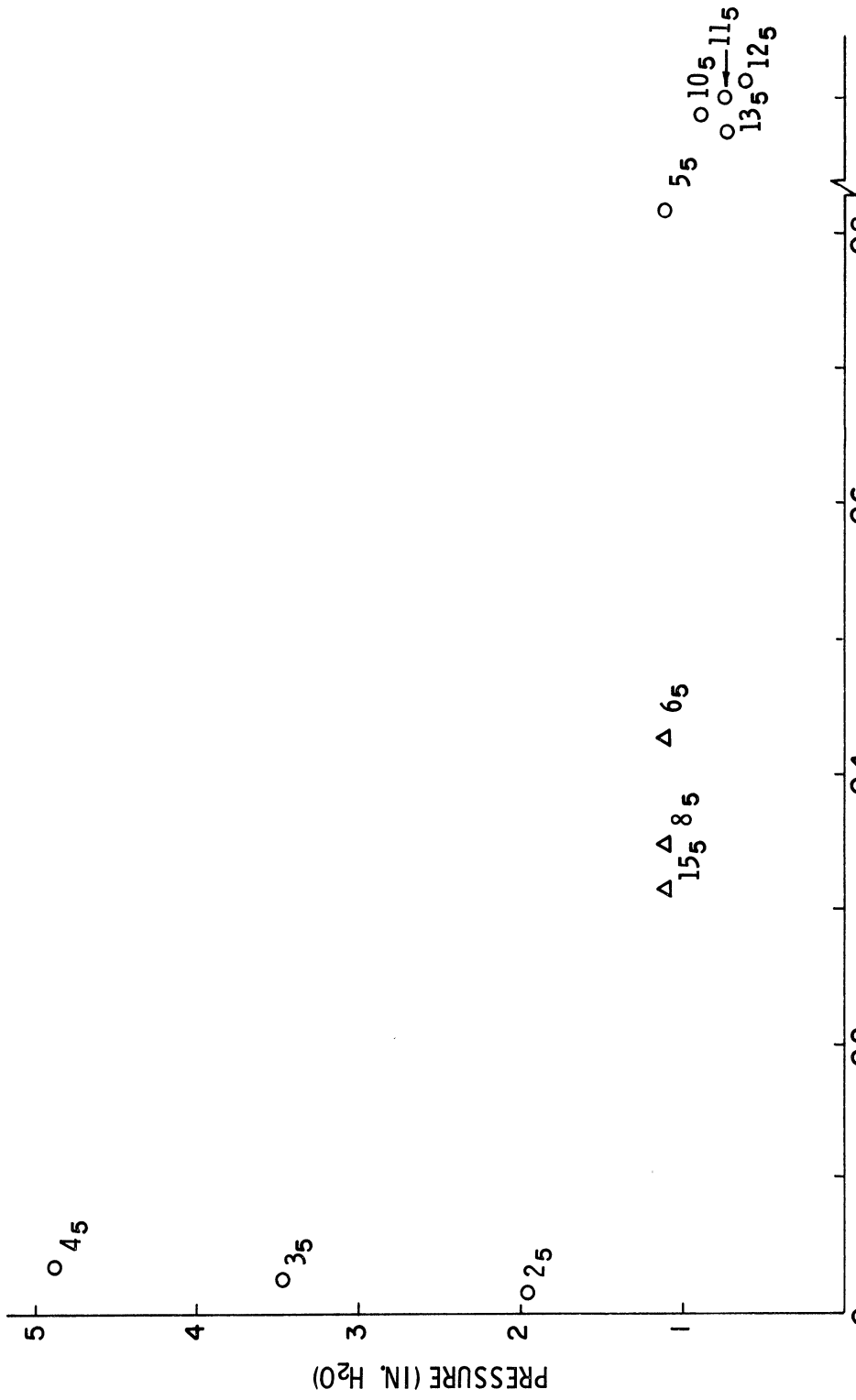

Fig. 10. Pressure vs. maximum radial displacement—Midwest shell No. 3 (0.100 in.), Test No. 5.

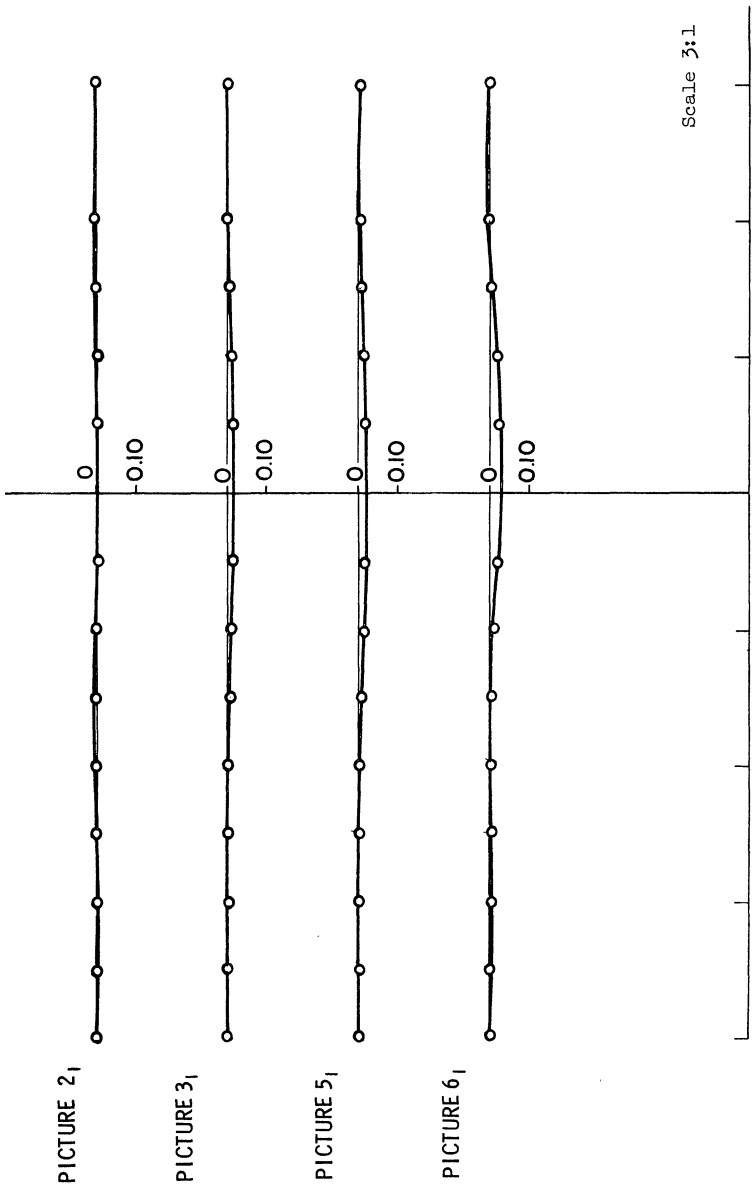

Fig. 11. Radial displacements—toy ball shell, Test No. 1.

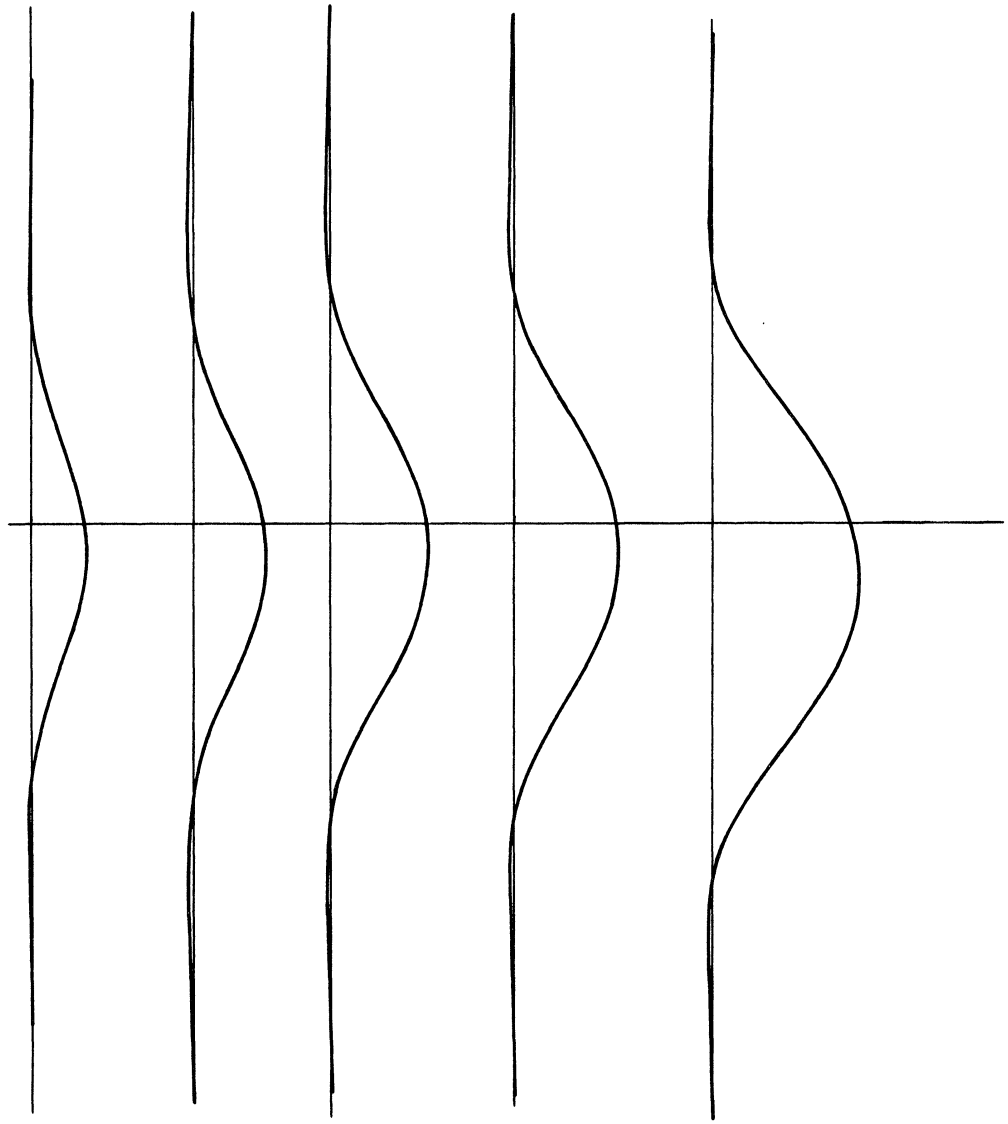

Fig. 11a. The radial displacements described by Eq. (6-1).

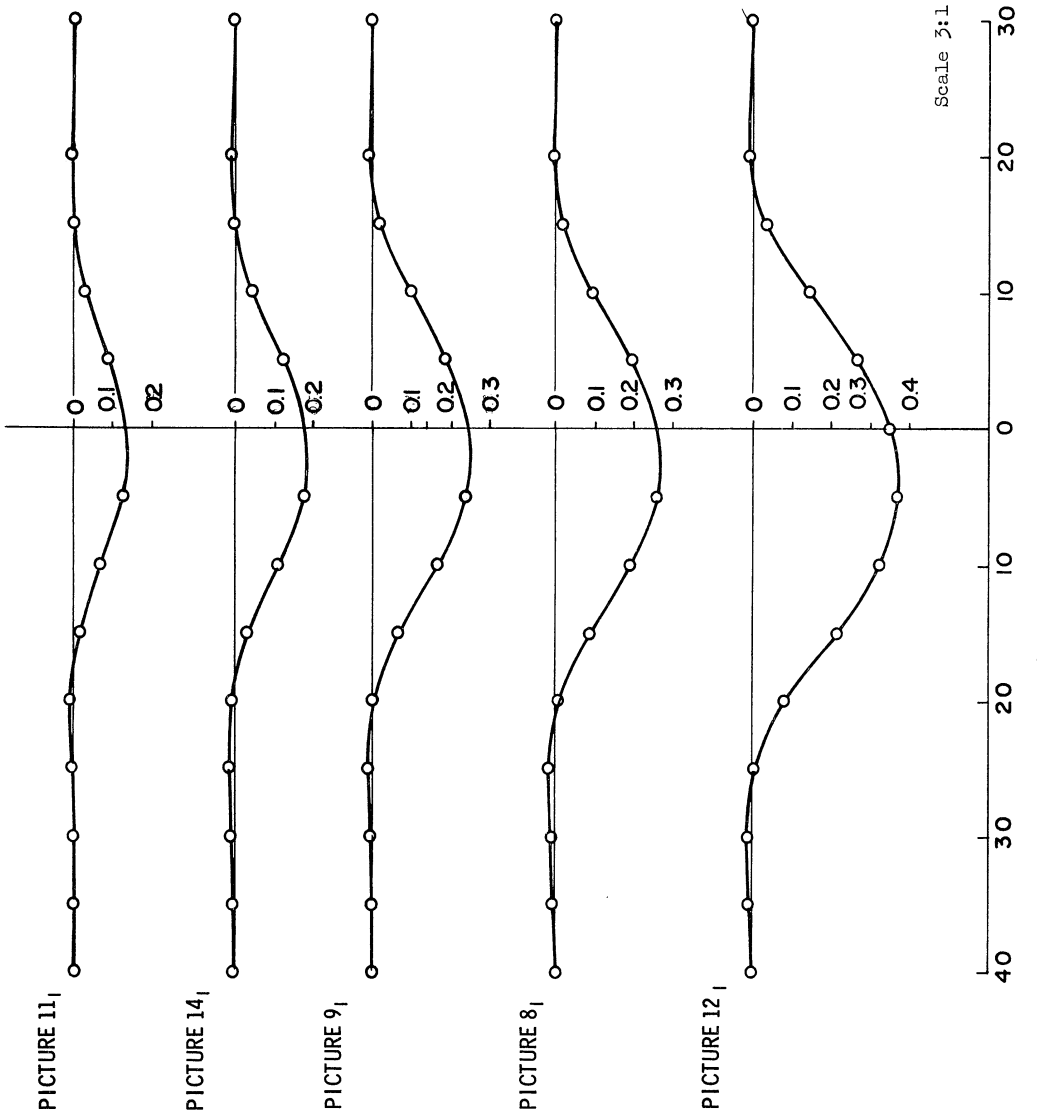

Fig. 11. (Concluded).

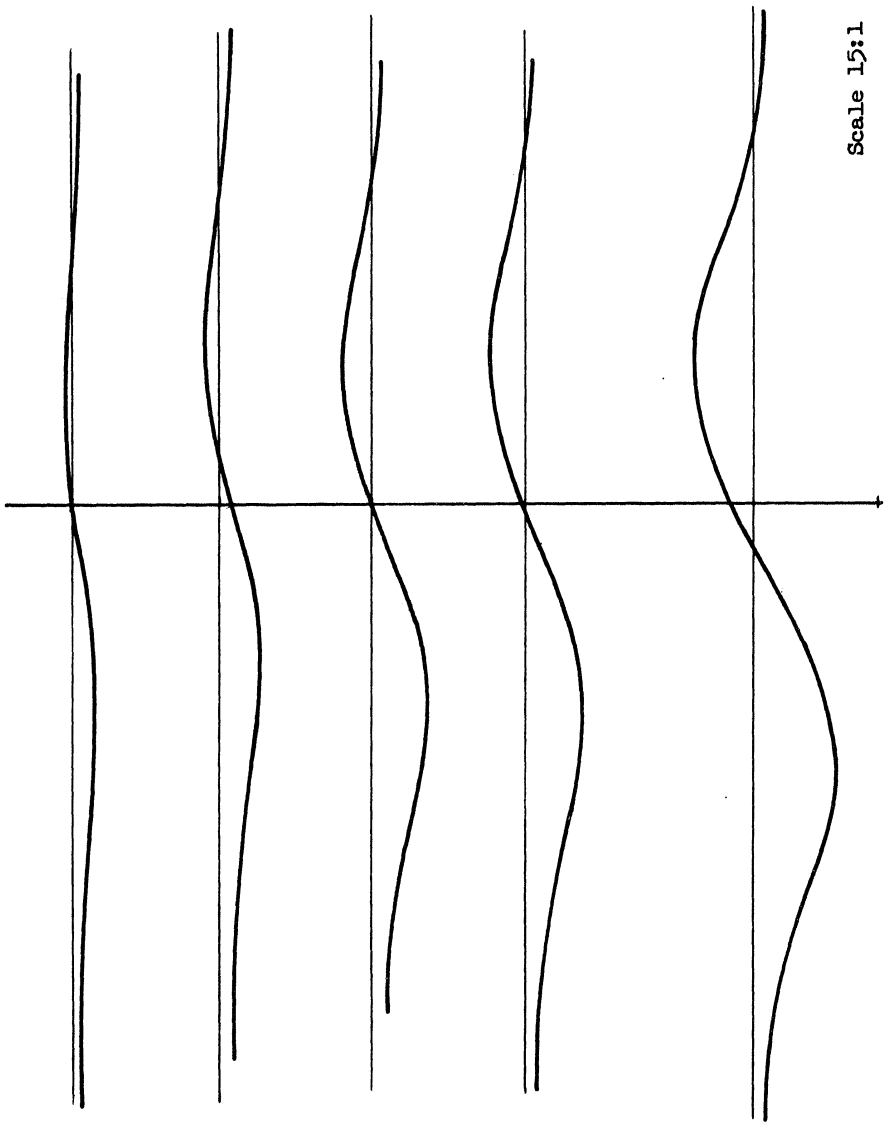

Fig. 12a. The tangential displacements described by Eq. (6-2).

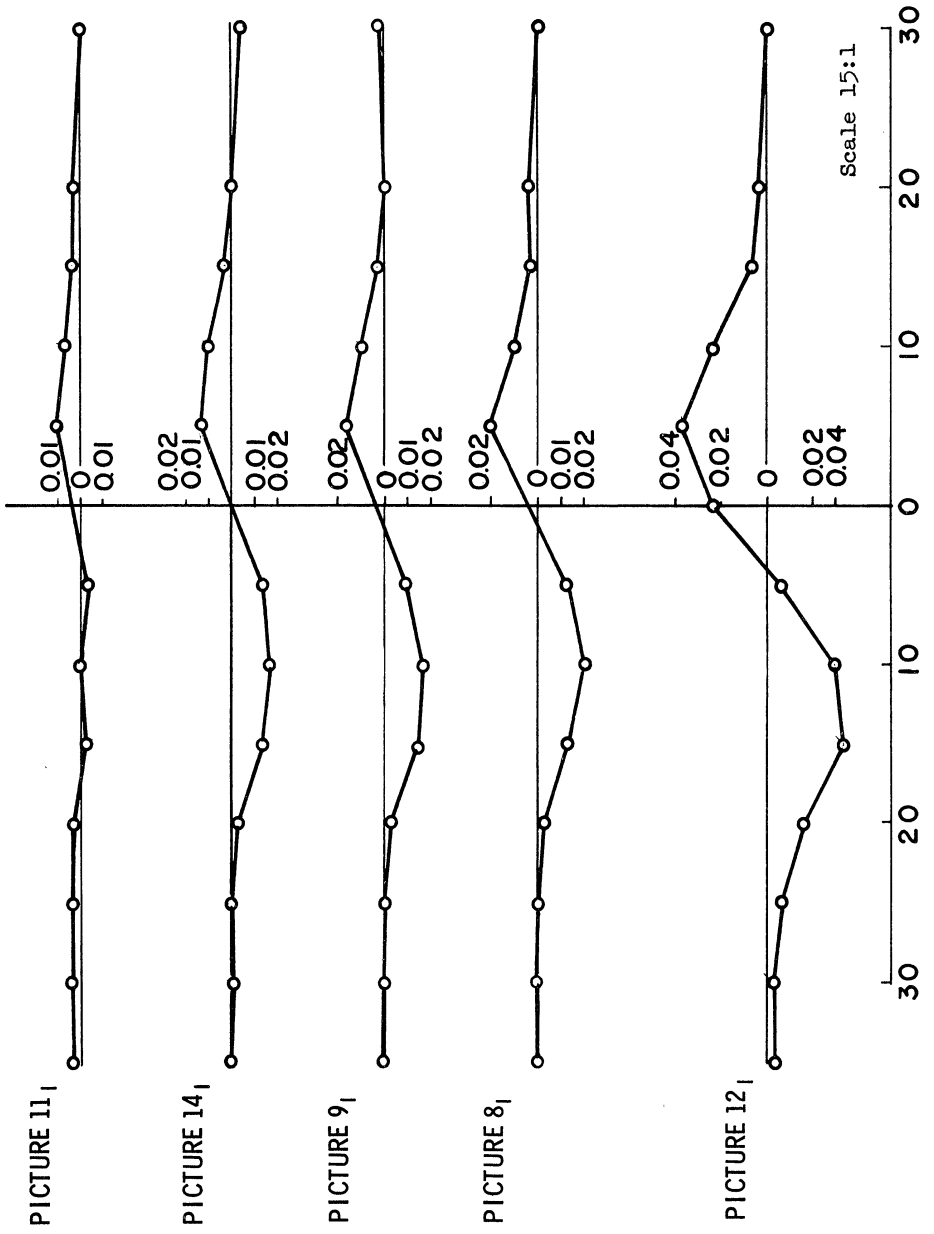

Fig. 12. Tangential displacements—toy ball shell, Test No. 1.

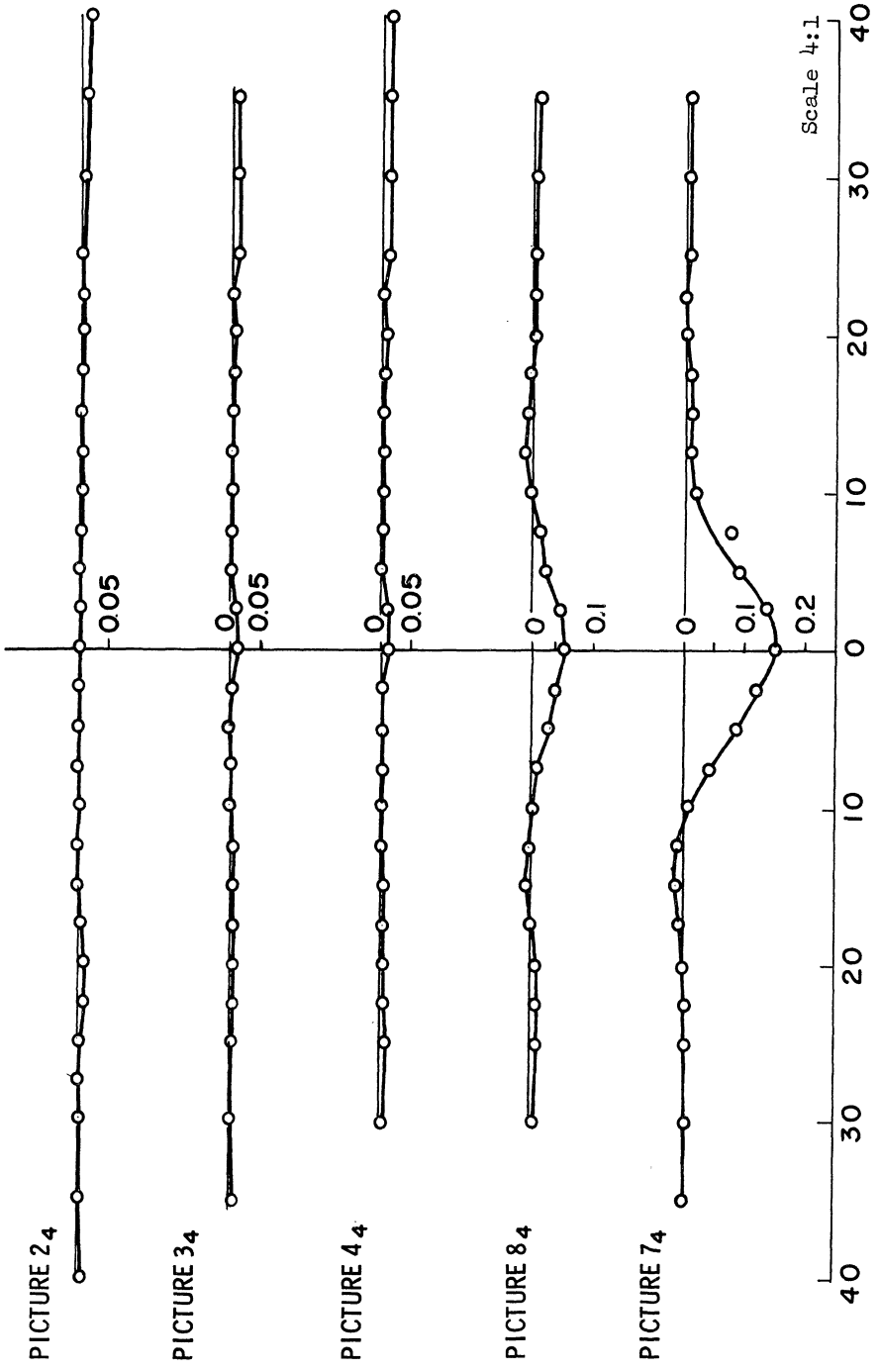

Fig. 13. Radial displacements—Midwest shell No. 1 (0.030 in.), Test No. 4.

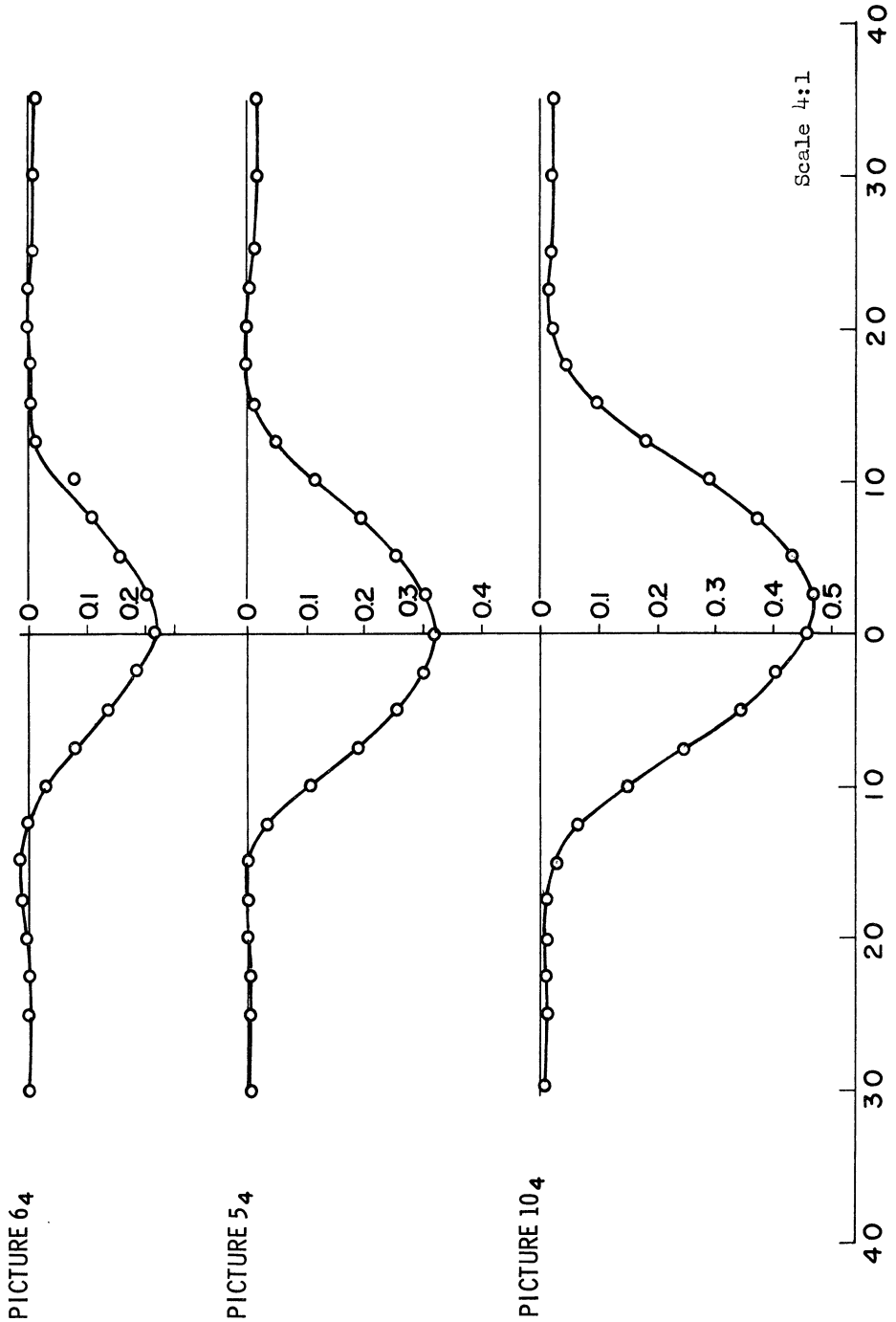

Fig. 13. (Continued).

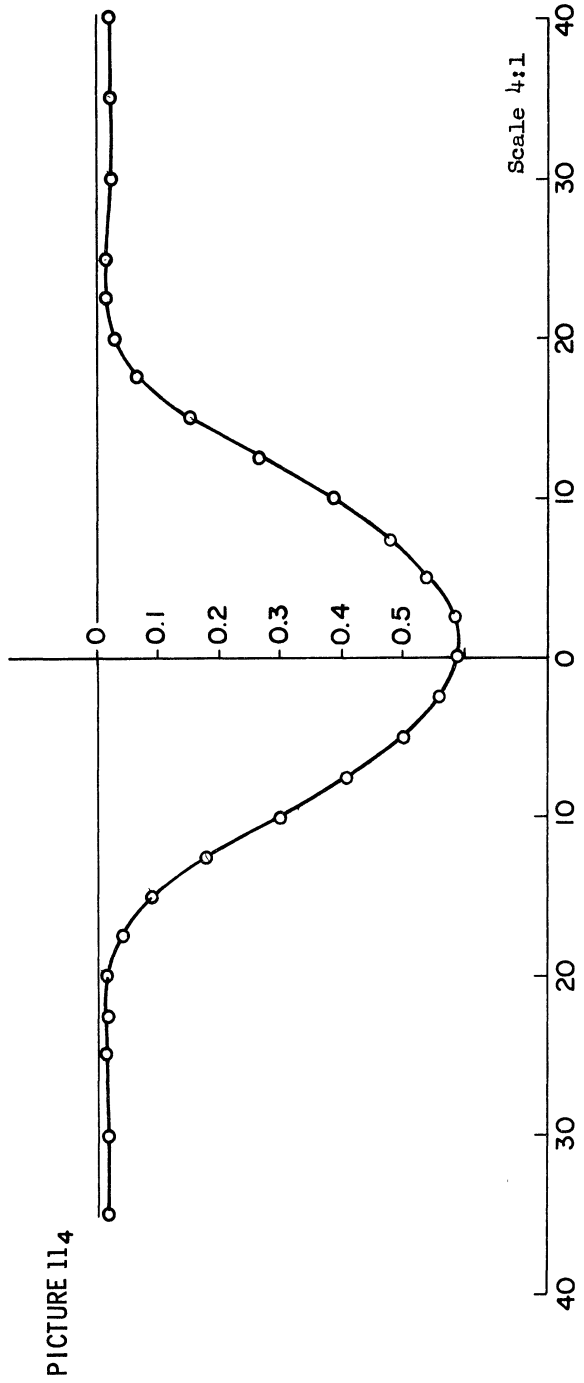

Fig. 13. (Continued).

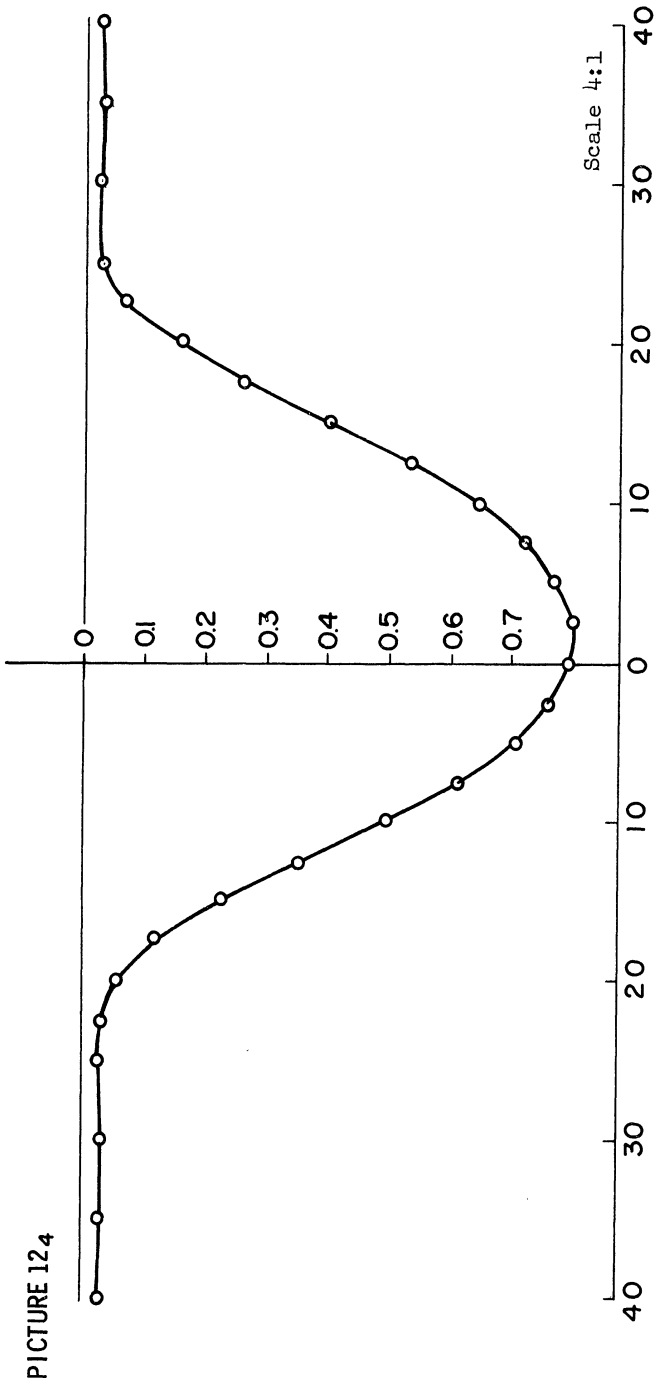

Fig. 13. (Continued).

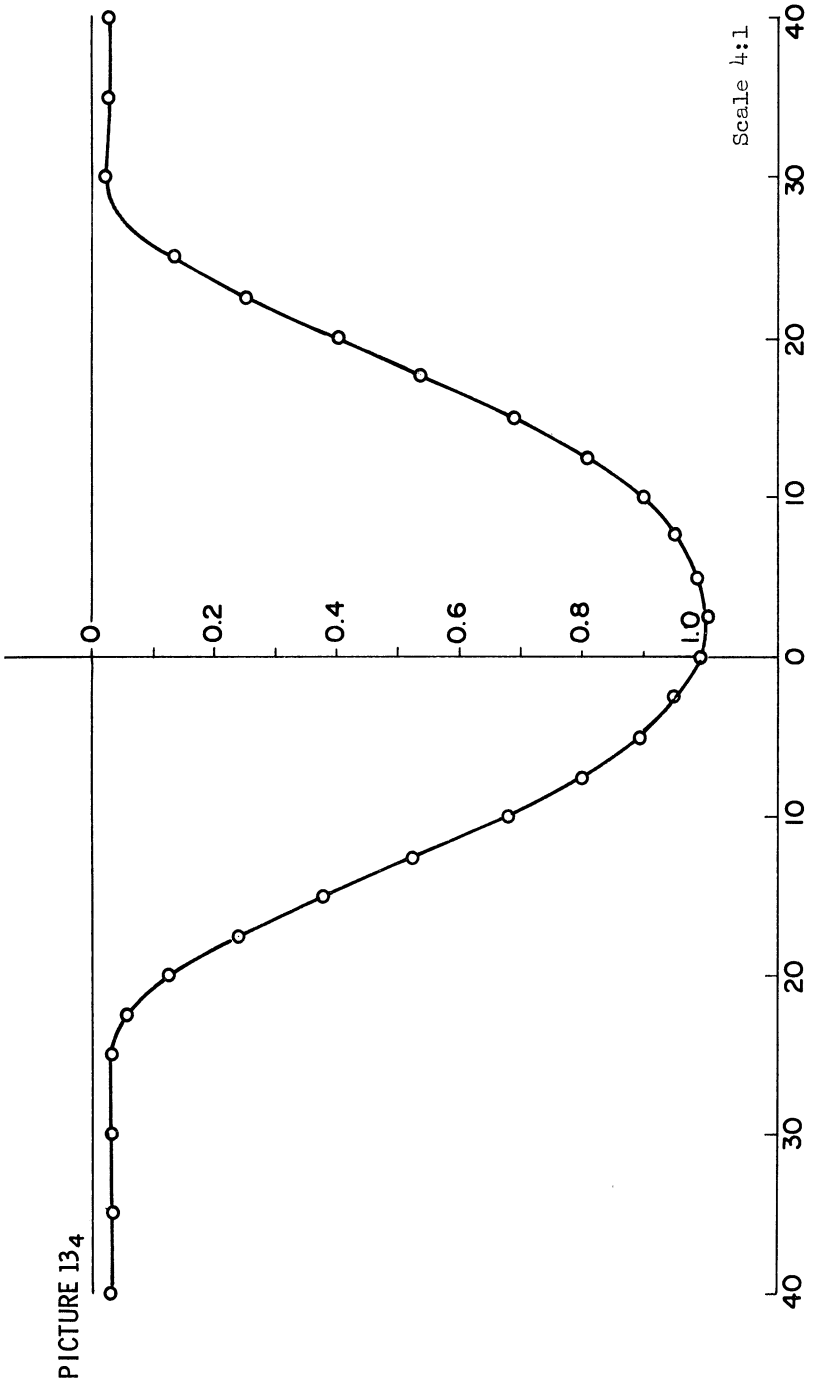

Fig. 13. (Continued).

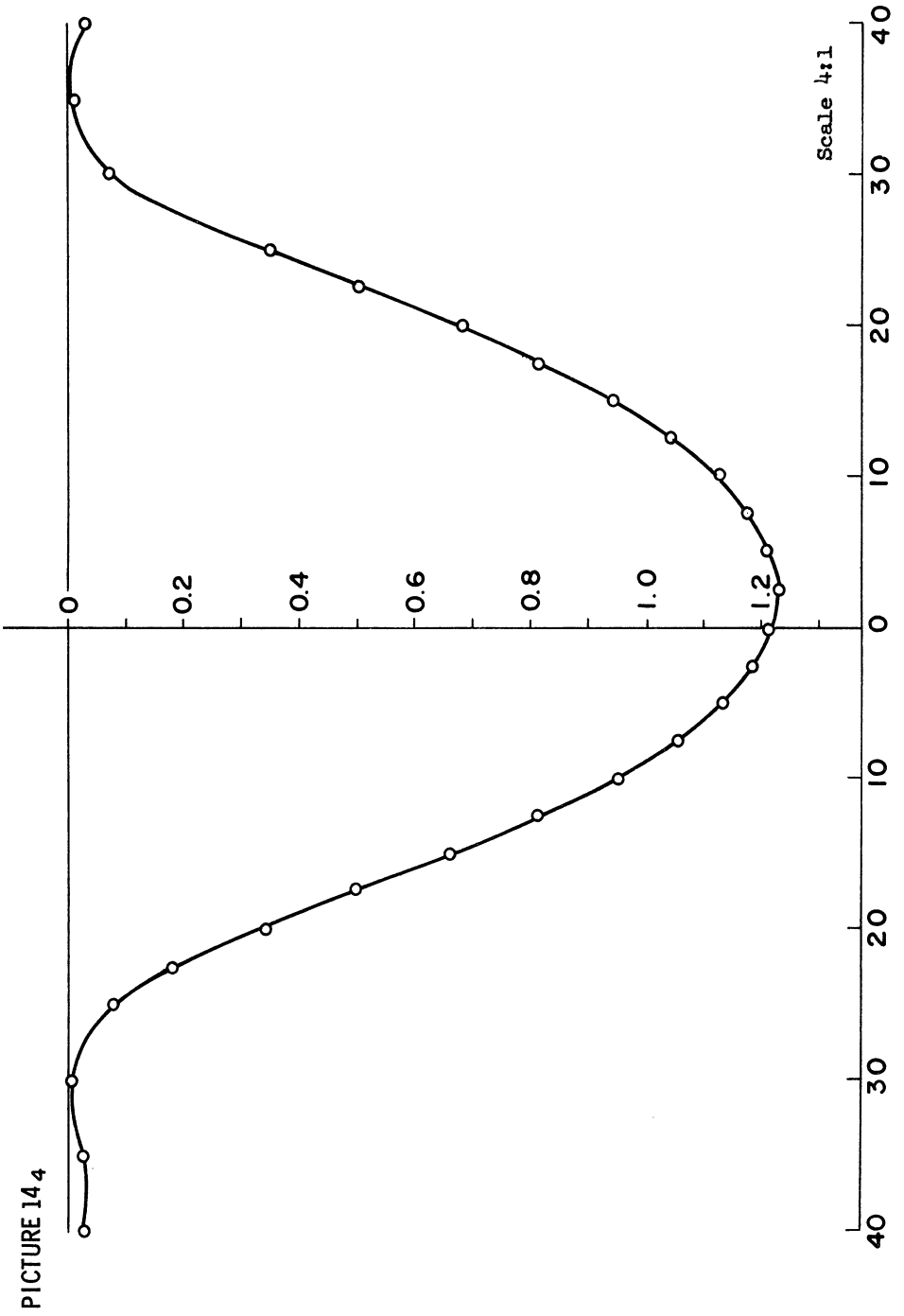

Fig. 13. (Concluded).

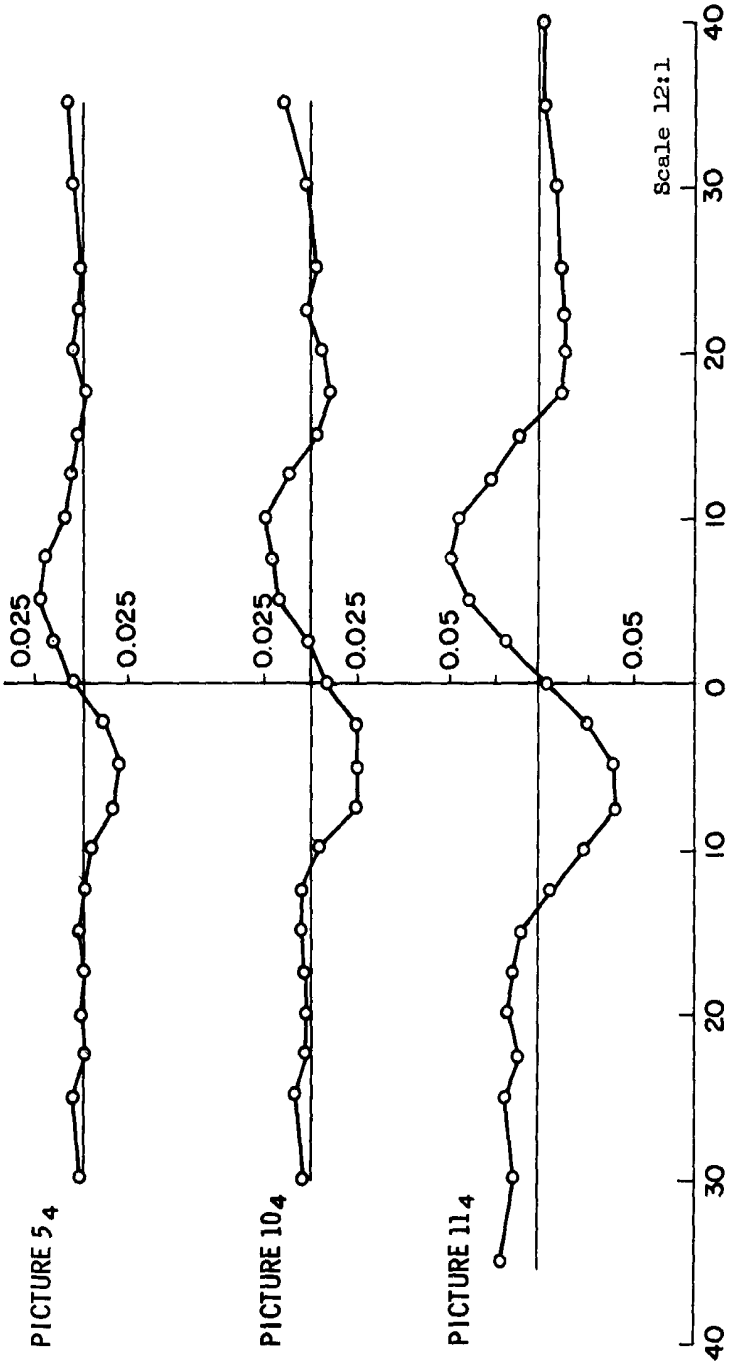

Fig. 14. Tangential displacements—Midwest shell No. 1 (0.030 in.), Test No. 4.

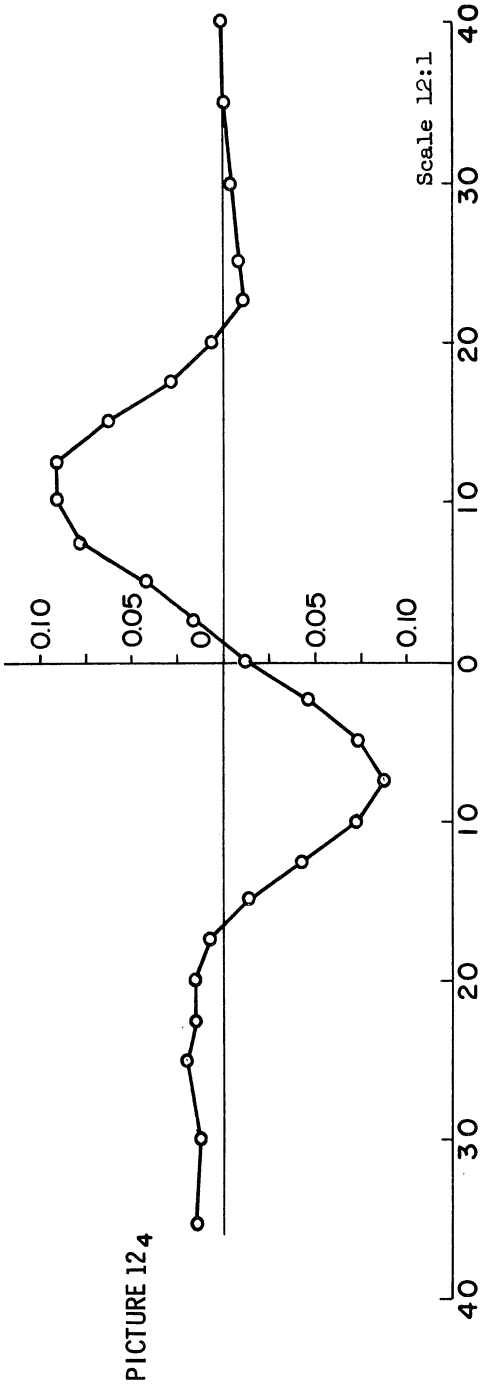

Fig. 14. (Continued).

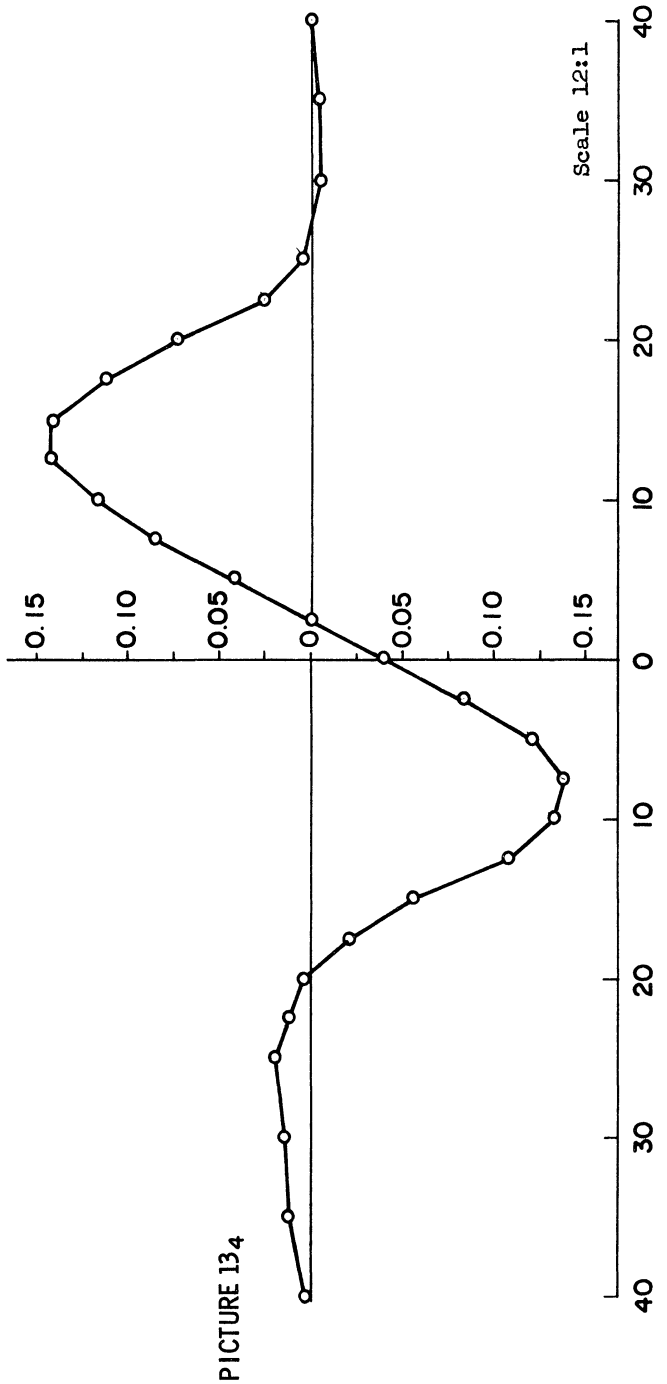

Fig. 14. (Continued).

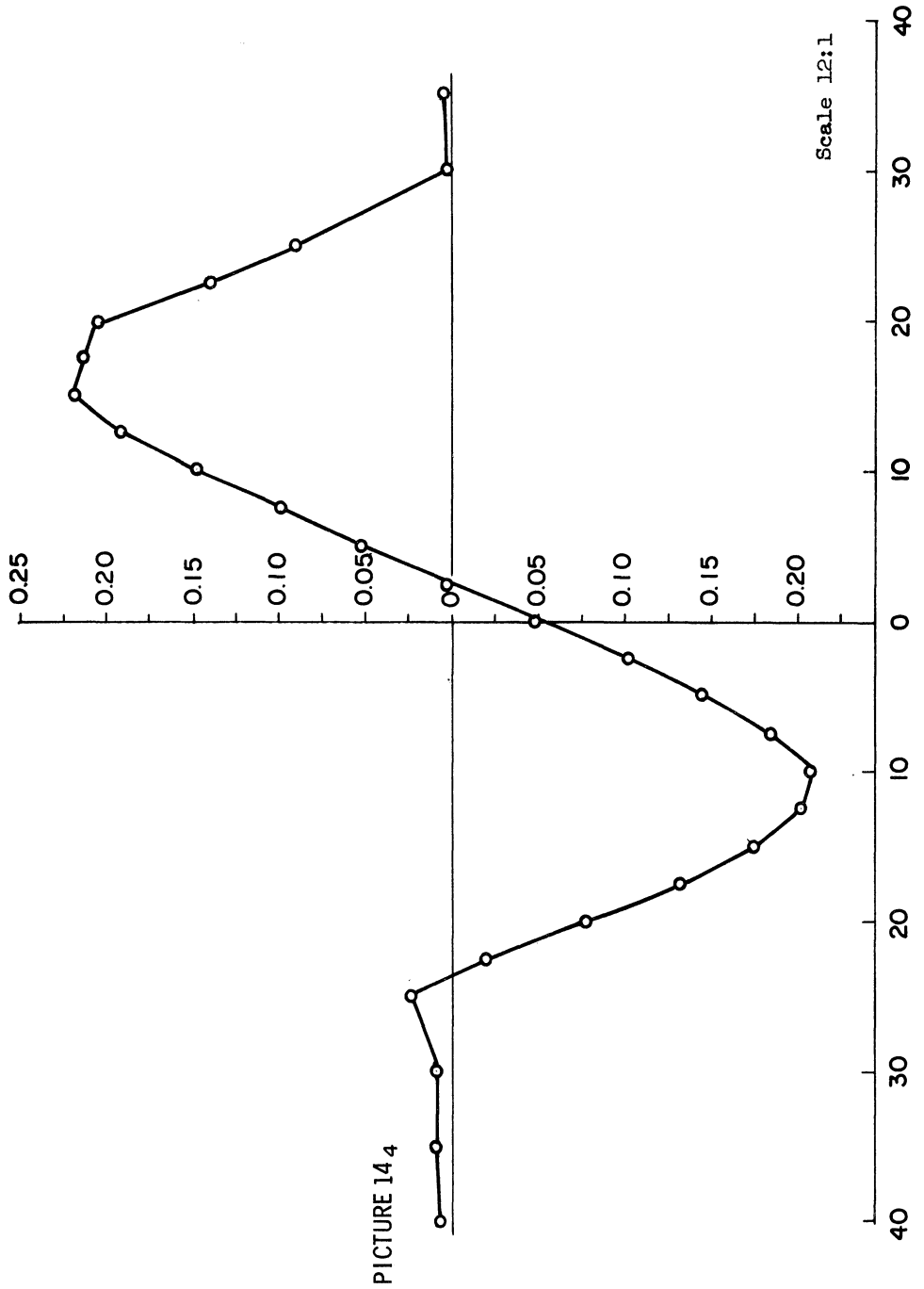

Fig. 14. (Concluded).

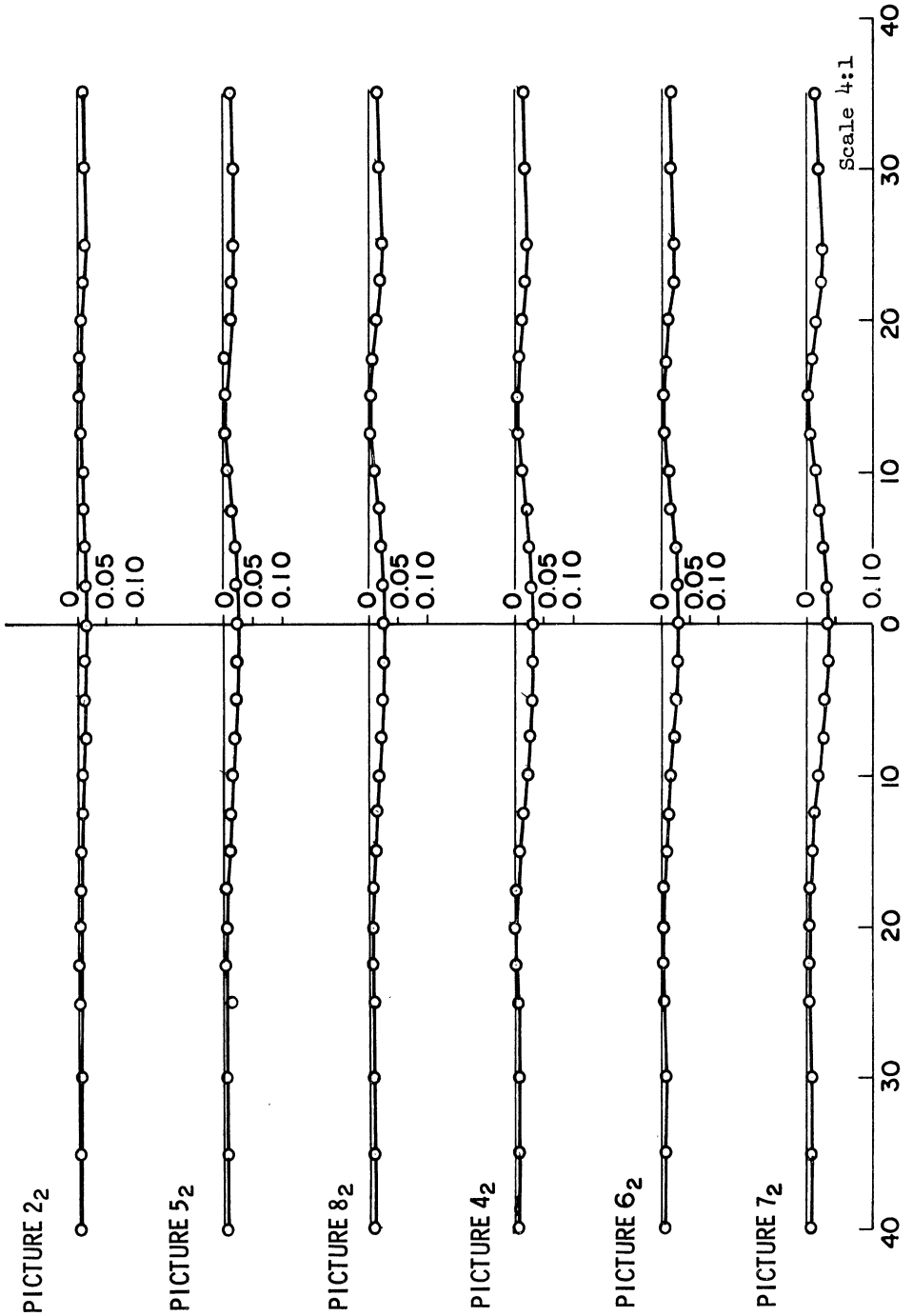

Fig. 15. Radial displacements—Midwest shell No. 2 (0.060 in.), Test No. 2.

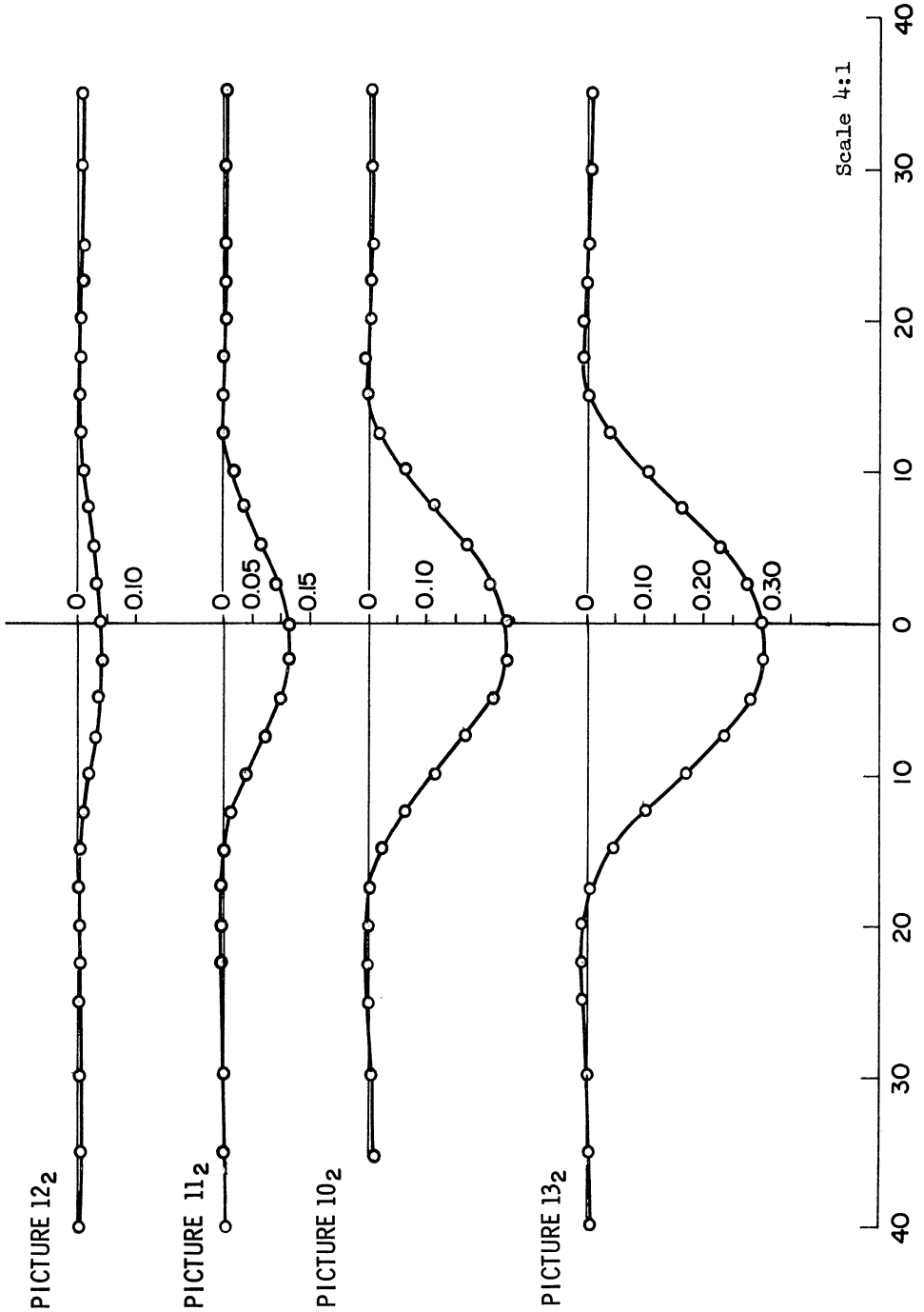

Fig. 15. (Continued).

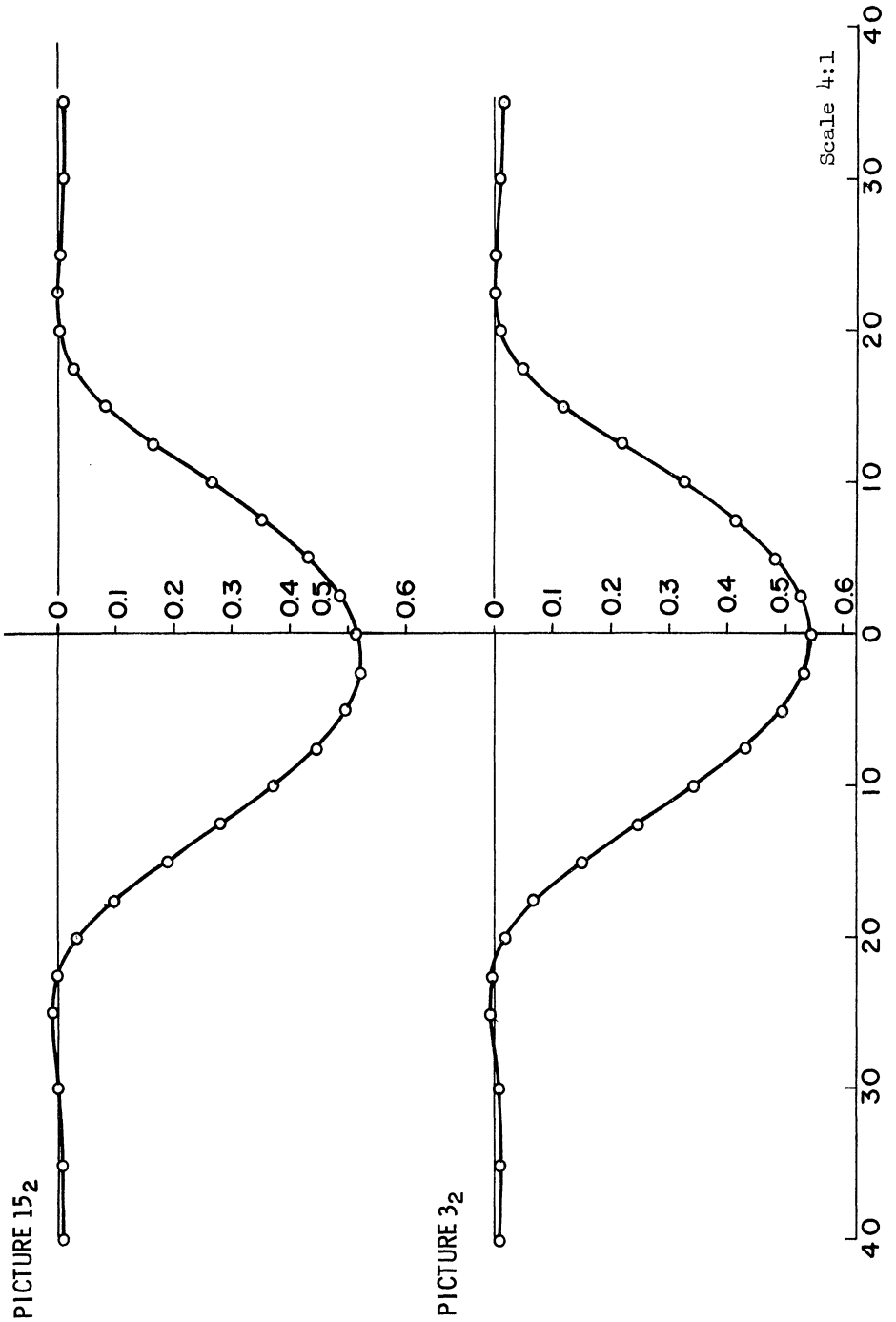

Fig. 15. (Continued).

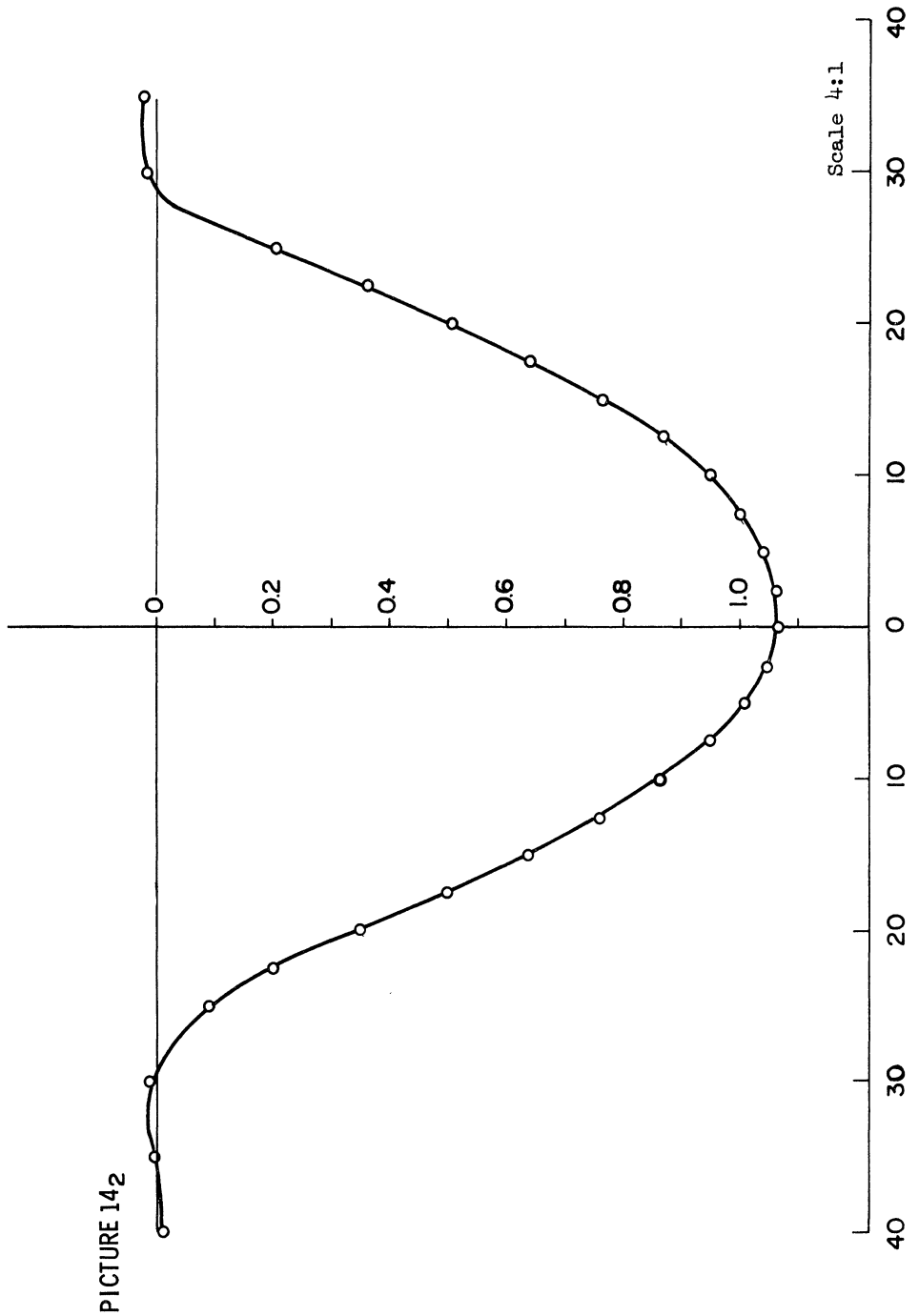

Fig 15. (Concluded).

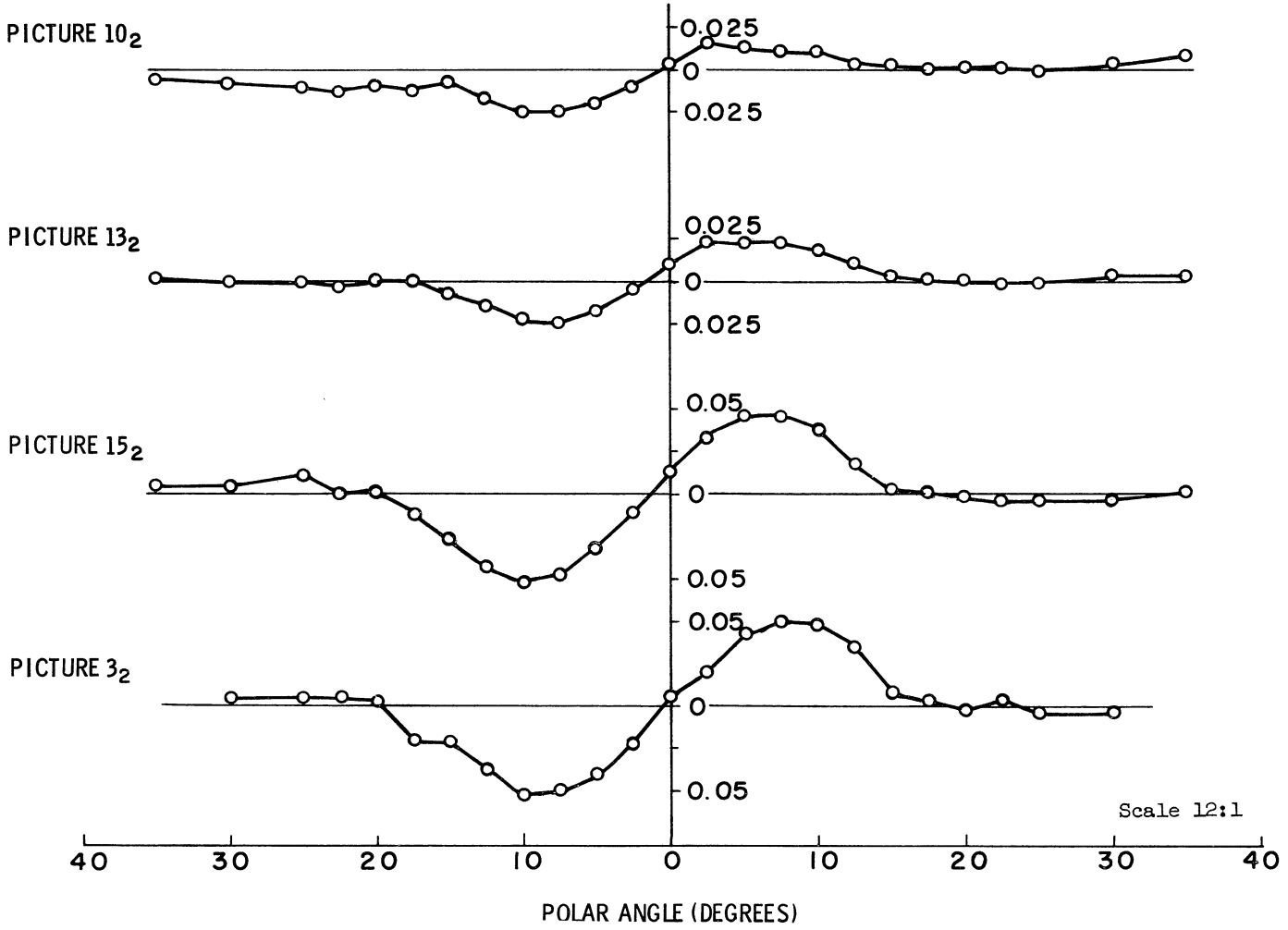

Fig. 16. Tangential displacements—Midwest shell No. 2 (0.060 in.), Test No. 2.

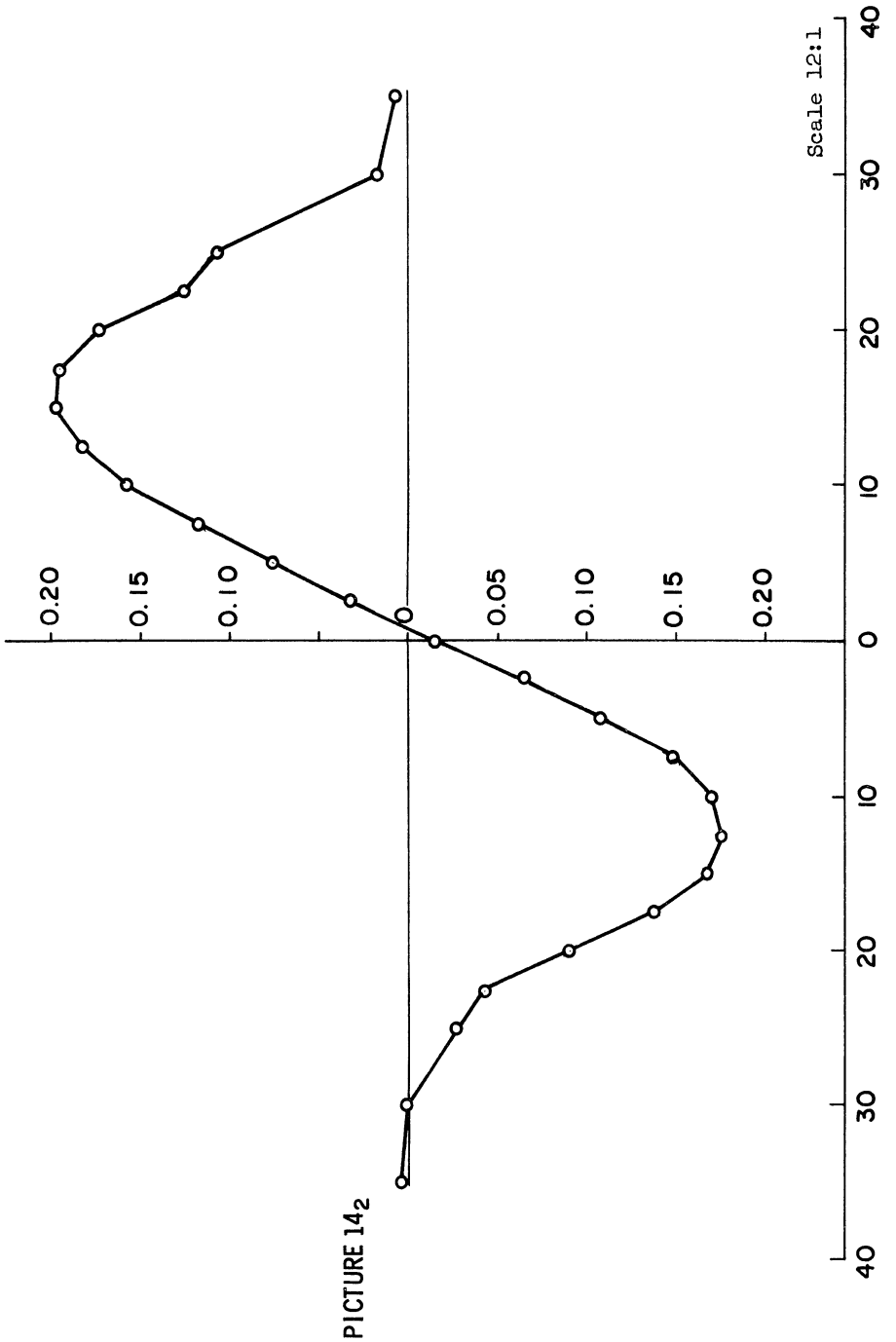

Fig. 16. (Concluded).

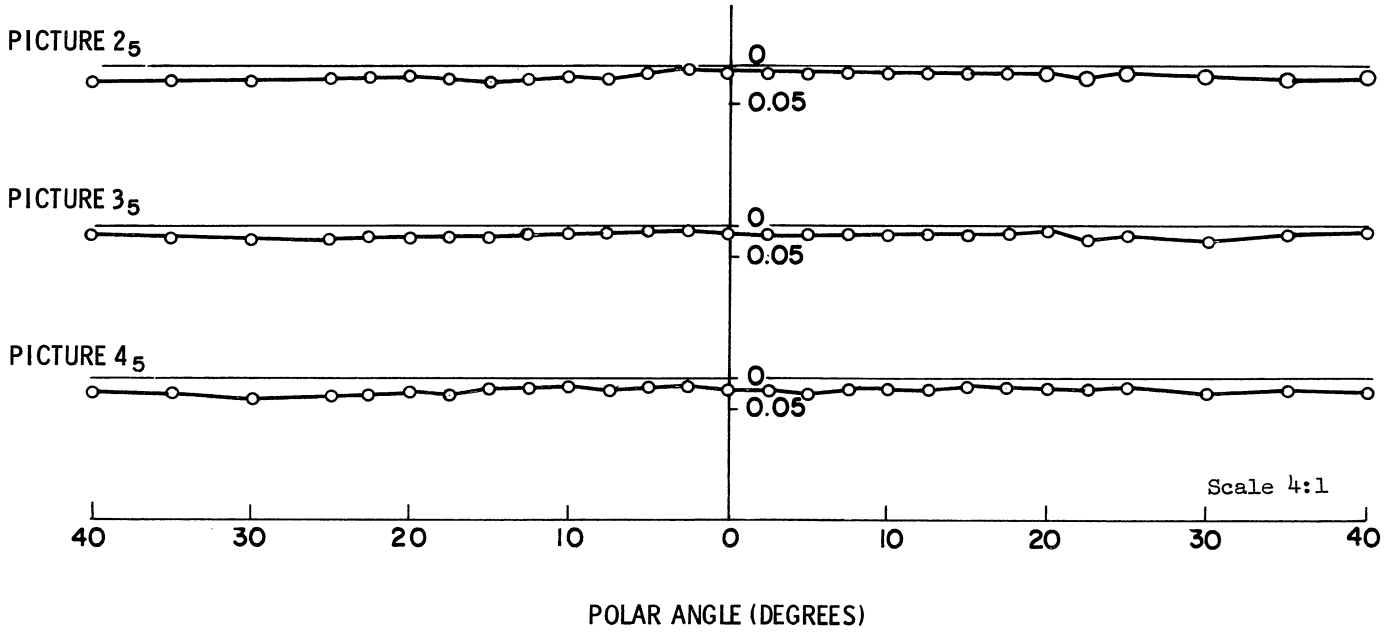

Fig. 17. Radial displacements—Midwest shell No. 3 (0.100 in.), Test No. 5.

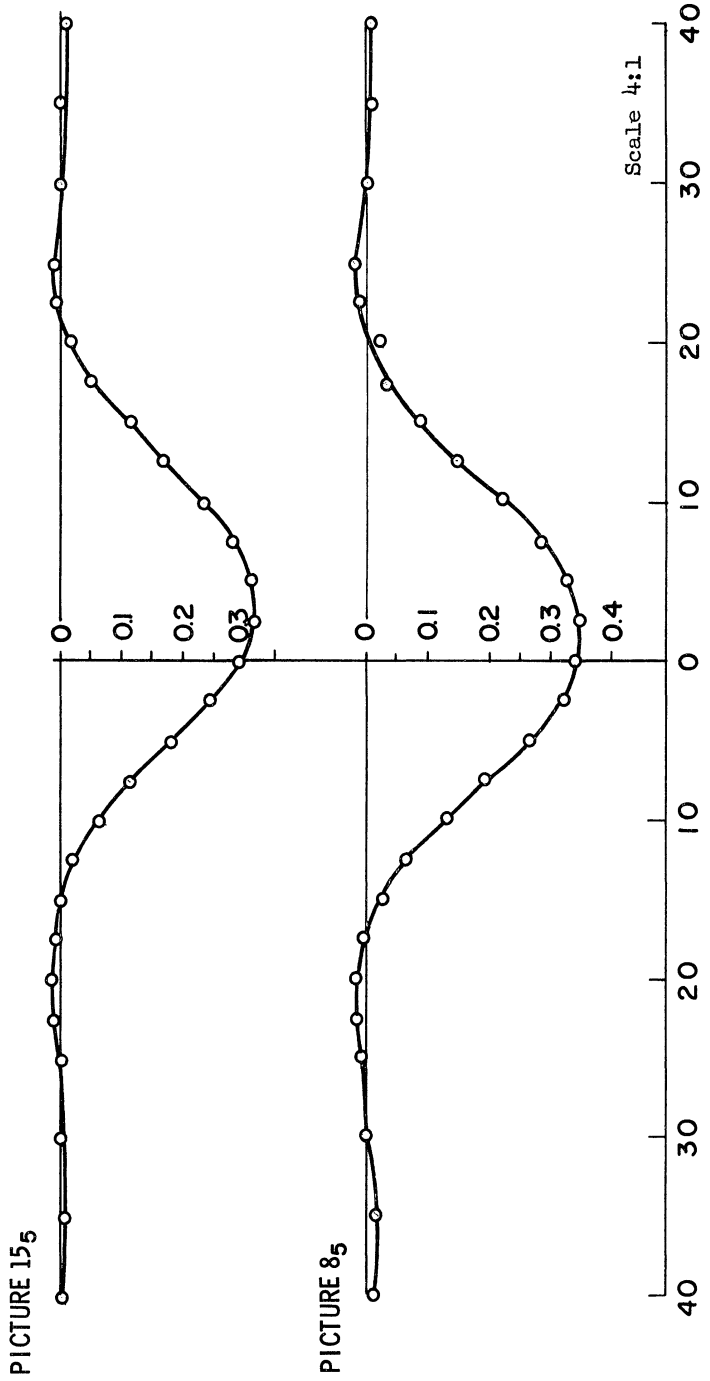

Fig. 17. (Continued).

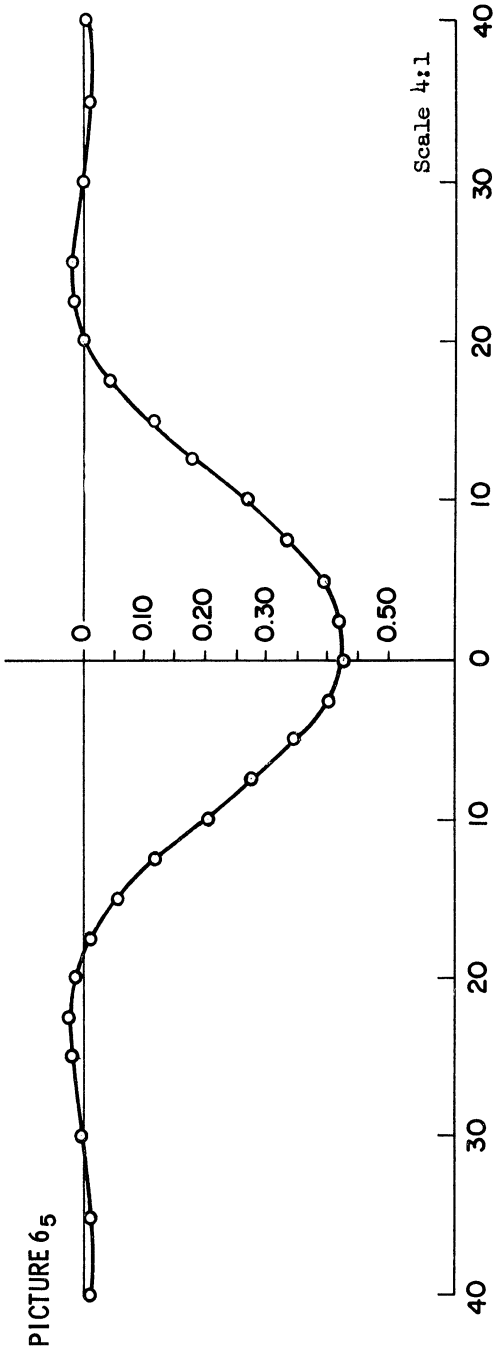

Fig. 17. (Continued).

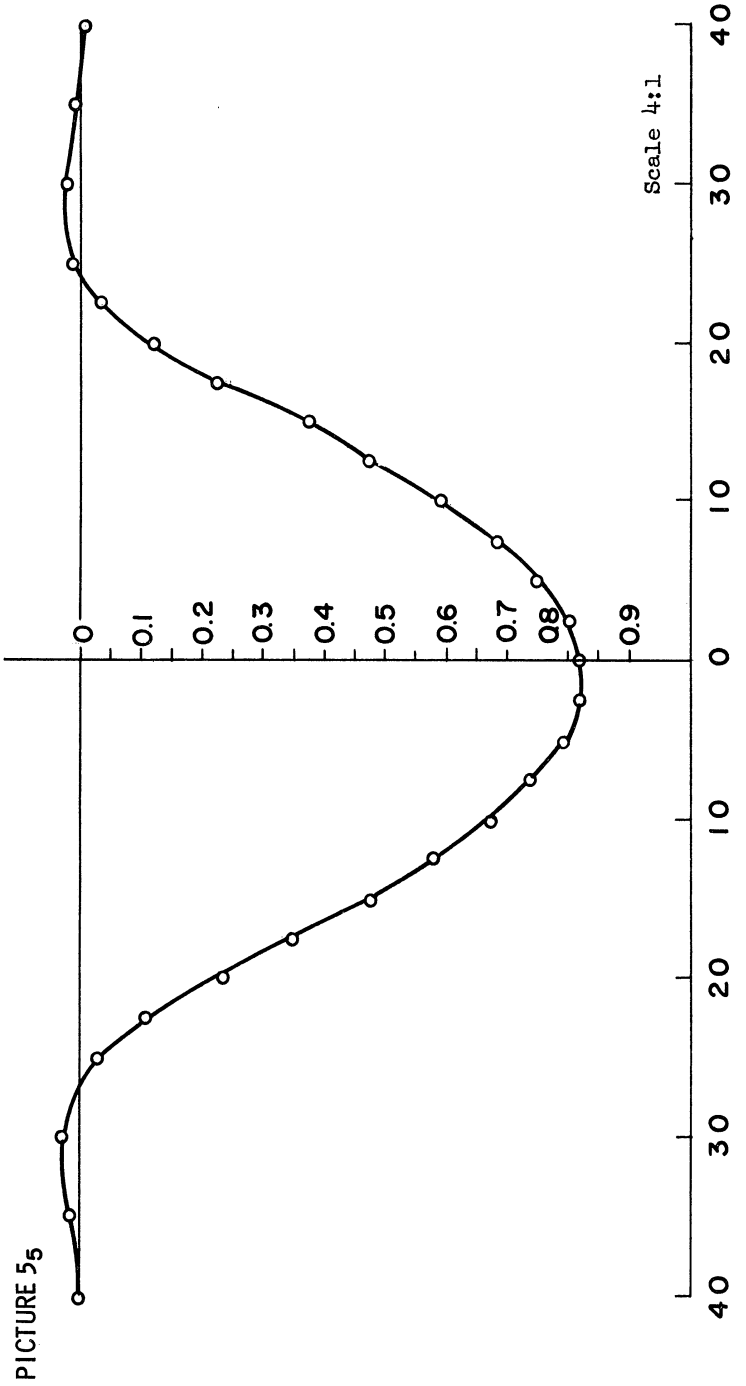

Fig. 17. (Concluded).

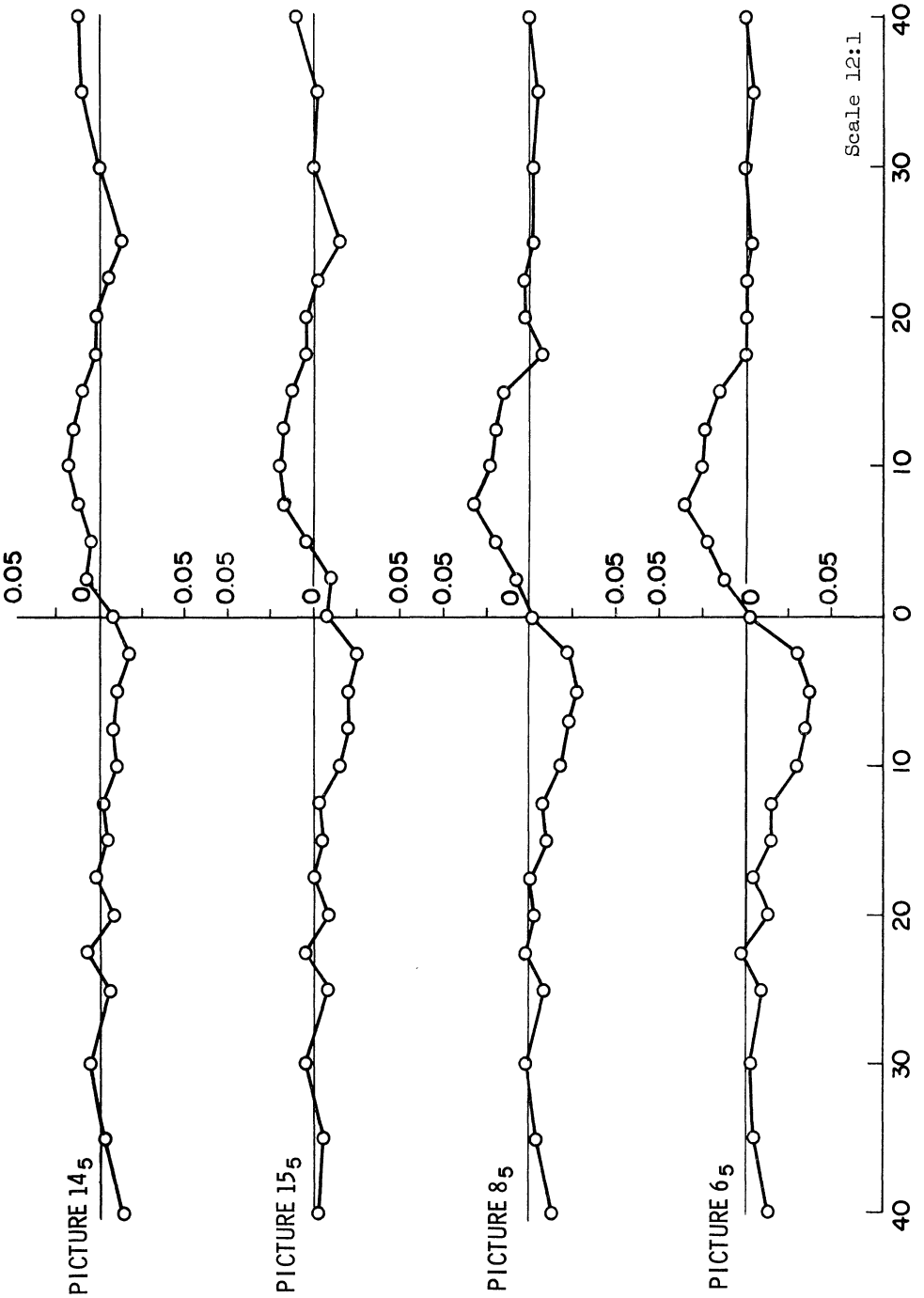

Fig. 18. Tangential displacements—Midwest shell No. 3 (0.100 in.), Test No. 5.

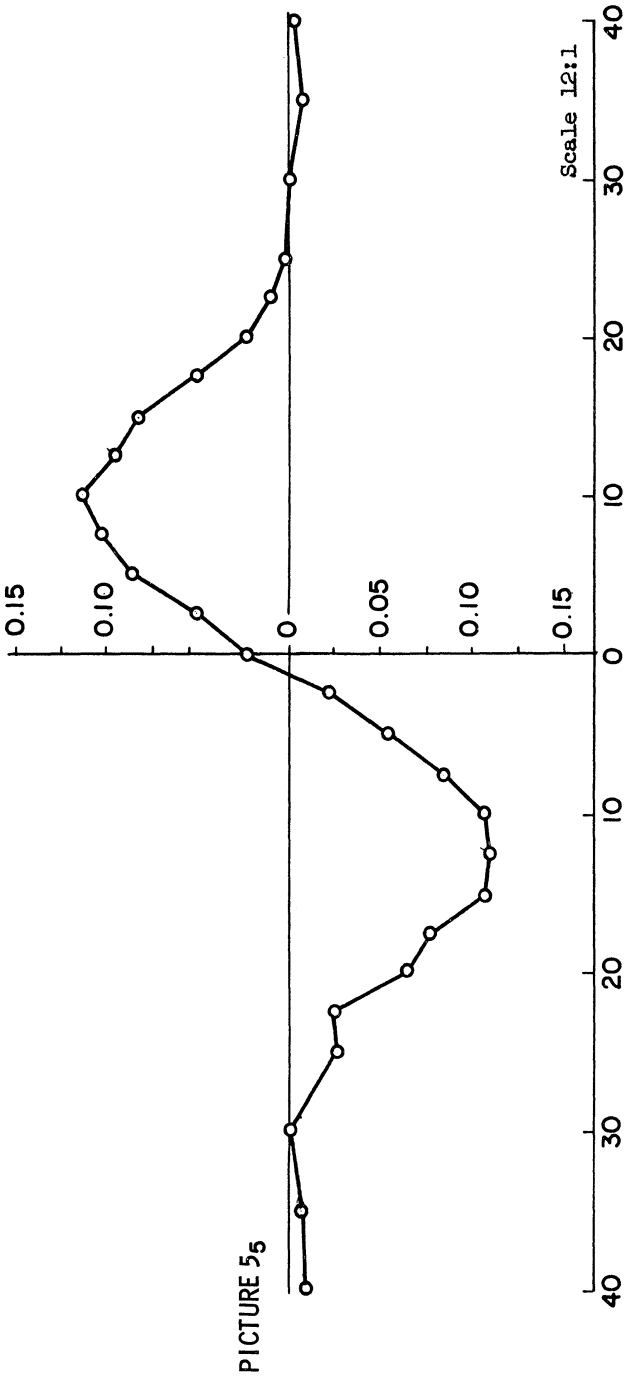

Fig. 18. (Concluded).